

## JGR Biogeosciences

## RESEARCH ARTICLE

10.1029/2019JG005438

## Key Points:

- An alkaline permeable reactive barrier was still efficient in removing inorganic contaminants in a wetland 10–11 years after installation
- Bacterial reduction, carbonate formation, sorption to colloids, and peat promoted U removal
- Near-neutral pH and anoxic conditions favored free ionic species of Co and Ni and promoted a more mobile speciation in peat and mineral soil

## Supporting Information:

- Supporting Information S1

## Correspondence to:

K. von Gunten,  
vongunte@ualberta.ca

## Citation:

von Gunten, K., Bishop, B., Zhang, L., Muehlenbachs, K., Alam, M. S., Konhauser, K. O., & Alessi, D. S. (2019). Biogeochemical behavior of metals along two permeable reactive barriers in a mining-affected wetland. *Journal of Geophysical Research: Biogeosciences*, 124, 3536–3554. <https://doi.org/10.1029/2019JG005438>

Received 27 AUG 2019

Accepted 30 SEP 2019

Accepted article online 19 OCT 2019

Published online 22 NOV 2019

## Author Contributions:

**Conceptualization:** Konstantin von Gunten


**Data curation:** Konstantin von Gunten

**Funding acquisition:** Kurt O. Konhauser, Daniel S. Alessi

**Investigation:** Konstantin von Gunten, Brendan Bishop, Luyu Zhang, Karlis Muehlenbachs, Md. Samrat Alam

**Methodology:** Konstantin von Gunten  
(continued)

## Biogeochemical Behavior of Metals Along Two Permeable Reactive Barriers in a Mining-Affected Wetland

Konstantin von Gunten<sup>1</sup> , Brendan Bishop<sup>1</sup>, Luyu Zhang<sup>1</sup>, Karlis Muehlenbachs<sup>1</sup>, Md. Samrat Alam<sup>1</sup>, Kurt O. Konhauser<sup>1</sup>, and Daniel S. Alessi<sup>1</sup>

<sup>1</sup>Department of Earth and Atmospheric Sciences, University of Alberta, Edmonton, Alberta, Canada

**Abstract** The biogeochemistry of two alkaline permeable reactive barriers (PRBs) installed for remediation in a mining-affected wetland was investigated in order to assess the importance of colloidal particles on metal removal processes in such systems. At the time of investigation, both PRBs were effective in removing U, Cu, and Zn (>95%) from groundwater but were slightly less efficient for Ni and Co (<90%). Previously installed groundwater wells allowed an in-depth analysis of groundwater passing through the first PRB. Here, in an alkaline environment (pH 6.0–9.7), 11–14% of Ni, 36–37% of Co, 77–81% of Cu, 14–17% of U, and 10–19% of Fe were associated with organic matter and inorganic colloids, while upgradient in the more acidic environments (pH <6.0), ionic species and complexes (e.g.,  $\text{Co}^{2+}$ ,  $\text{Ni}^{2+}$ ,  $\text{Cu}^{2+}$ , and  $\text{UO}_2\text{H}_3\text{SiO}_4^+$ ) dominated. Copper and U preferentially bound to larger colloidal fractions (>1 kDa), which might have promoted their sequestration. Uranium removal was likely further enhanced by U (VI) reduction in the alkaline and oxygen-depleted conditions of the PRBs. The less efficient removal of Ni and Co, being target metals for remediation, was explained by a combination of their high solubility, unfavorable redox and pH conditions created by the alkaline PRBs, and their limited association with colloidal particles. These considerations are critical in the design of future PRBs for the remediation of similar systems.

**Plain Language Summary** Permeable reactive barriers are a technology often applied to treat contaminated groundwater. In this study, the biogeochemistry of two alkaline barriers, placed in a wetland near a decommissioned uranium mine, was investigated. At the time of investigation, both reactive barriers were effective in removing uranium, copper, and zinc from groundwater but were less efficient for nickel and cobalt. Using previously installed groundwater wells, we conducted an in-depth analysis of groundwater passing through the first barrier. The alkaline and oxygen-depleted environment promoted the formation of colloids, which potentially contributed to the effective removal of copper and uranium, while the surrounding acidic wetland promoted the transport of ionic metal species. At the reactive barriers, uranium removal was further enhanced by uranium reduction to more immobile uranium forms through reduced chemical species and the activity of bacteria. The less efficient removal of nickel and cobalt was explained by their high solubility, unfavorable conditions created by the alkaline reactive barriers, and their limited association with colloids. This work provides new insights into future uses of permeable reactive barrier technology for metal remediation in wetlands.

## 1. Introduction

Permeable reactive barriers (PRBs) are an in situ technology applied to the remediation of both organic and inorganic contaminants in groundwater (Powell et al., 1998). Typically, a trench is excavated perpendicular to the flow of contaminated groundwater and then backfilled with a mixture of reactive and permeable material. Contaminants are removed by sorption or precipitation, or, if the contaminant is organic, they are degraded by redox processes (Blowes et al., 2000; Powell et al., 1998). Several authors have investigated the use of PRBs to treat inorganic contaminants (e.g., Benner et al., 1999), yet few studies document PRB performance in cold climates (e.g., Snape et al., 2001) or the use of limestone and lime as reactive mediums to treat inorganic contamination (e.g., Golab et al., 2006). The transport behavior of trace metals in aqueous environments is strongly affected by redox conditions, pH, available ligands (e.g., organic acids), and potential sorption sites (Borch et al., 2010; Violante et al., 2010). However, colloidal particles (1–1,000 nm and up to 10  $\mu\text{m}$  in some environments), which are little affected by gravitational setting, can substantially alter the transport behavior of trace metals (Dai et al., 1995; Gustafsson & Gschwend, 1997; Honeyman, 1991).

**Project administration:** Konstantin von Gunten, Kurt O. Konhauser, Daniel S. Alessi

**Resources:** Karlis Muehlenbachs

**Supervision:** Konstantin von Gunten, Md. Samrat Alam, Kurt O. Konhauser, Daniel S. Alessi

**Validation:** Konstantin von Gunten

**Visualization:** Konstantin von Gunten

**Writing - original draft:** Konstantin von Gunten, Kurt O. Konhauser, Daniel S. Alessi

**Writing - review & editing:**

Konstantin von Gunten

Despite this, few studies have investigated the importance of colloidal transport of trace metals in mining-affected wetlands (e.g., Wang et al., 2013) and their importance in the performance of PRBs.

In this study, we investigated metal speciation and mobility along PRBs installed in a wetland (fen type) at a decommissioned mine in Cluff Lake, northern Saskatchewan, Canada (Figure 1), that was reported to receive inputs of U, Mn, Fe, Ni, Co, and Zn and traces of Cu and Mo due to previous mining activities (von Gunten et al., 2018). The wetland is characterized by a 0- to 2-m-thick peat cover overlying a 2- to 7-m-thick sandy till (Canadian Nuclear Safety Commission, 2003). Major vegetation consists of *Sphagnum* spp., *Polytrichum* sp., *Drosera rotundifolia*, *Carex* spp., and various shrubs, including *Salix bebbiana*, *Salix candida*, *Alnus crispa*, and *Betula occidentalis*. The two experimental PRBs were designed and installed in 2006 and 2007 by the site owner to intercept a waste stream found to originate at the “Claude” waste rock pile northeast of the wetland. The goal was to reduce contaminant flow into a nearby stream, with a major focus on the removal of U. A local hydrogeological model (refer to AREVA, 2013, p. 360) indicated groundwater flow from northeast of the wetland toward the southwest. The 2006 PRB (PRB2) contained a mixture of gravel (50%) and peat (50%) with additions of lime and limestone (unknown amounts). The 2007 PRB (PRB1) was installed further upgradient of groundwater flow and was backfilled with gravel (60%), peat (35%), lime (3%), and limestone (2%). The dimensions of PRB2 are not well documented, but it is longer but narrower compared to the PRB1, which was originally 124 m long, 2 m wide, and 4–9 m deep (see Figure S1 in the supporting information for photos). A previous study showed that the reactive barriers efficiently removed U, which was one of the major metals of concern in the groundwater. However, the barriers did not remove Co and Ni to a similar extent, which, given their potential toxicity, was considered as problematic (AREVA, 2013). Nevertheless, the wetland itself successfully diminished metal concentrations further downgradient of the PRBs. The reasons for the suppressed performance of the PRBs in regard to Co and Ni were not further investigated by the site owner.

In order to better understand how biogeochemical factors, and in particular the role of colloidal metal associations, could affect the barrier performance and metal removal, we applied geochemical modeling and colloidal analyses (using filtrations and asymmetrical flow field flow fractionation, or AF4) on groundwater samples, as well as metal speciation investigations (using sequential extractions) and 16S rRNA gene sequencing on soil samples to obtain an integrated understanding of the PRB environment. The results from this study provide vital information for future mining waste management scenarios and for PRB designs in similar environments.

## 2. Materials and Methods

### 2.1. Peat and Soil Samples

All sampling was organized along a transect passing through both PRBs and utilizing existing groundwater wells (Figure 1). In 2017, surface samples were collected along a transect in the direction of groundwater flow to a depth of 20–30 cm (“surface,” S) using a hand auger 2 m away from nearby wells (wells 11, 13, 15, 20, 5, 22, and 24) and perpendicular to the groundwater flow. At PRB1, an additional 90- to 100-cm-deep sample was collected (15D). In 2018, at selected locations, deeper soil samples from the peat/mineral soil interface were collected, for which depth at the sampling locations varied between 110 and 210 cm (Table 1). All peat/soil samples were placed into plastic bags and sealed for transportation.

In the laboratory, subsamples of the collected peat and soil were dried (105 °C) to determine the water content by mass loss. The dried samples were then ground by a mortar and pestle and analyzed for total carbon, total organic carbon (TOC), and total nitrogen using a Thermo Scientific Flash 2000 elemental analyzer at the University of Alberta (UofA). Mineralogy of the mineral soil samples and all samples taken from PRB1 (15S, 15D, and 15M) were determined at the UofA with an Ultima IV X-ray diffraction (XRD) unit (Rikagu) with a cobalt X-ray source ( $\lambda = 1.790260$ ) using the JADE 9.5 software packages and databases (2013 ICDD and 2015-1 ICSD) for interpretation. Samples from the PRB were also separated through a set of sieves (2, 1, and 0.075 mm) to determine the size distribution of the upper layers. The pH of selected samples was measured in a water slurry using a 1:5 mass-to-volume ratio using air dried, ground, and sieved (<2 mm) solids (Rayment & Higginson, 1992), which require hand squeezing for wetted peat samples due to their high water absorption (Stanek, 1973).

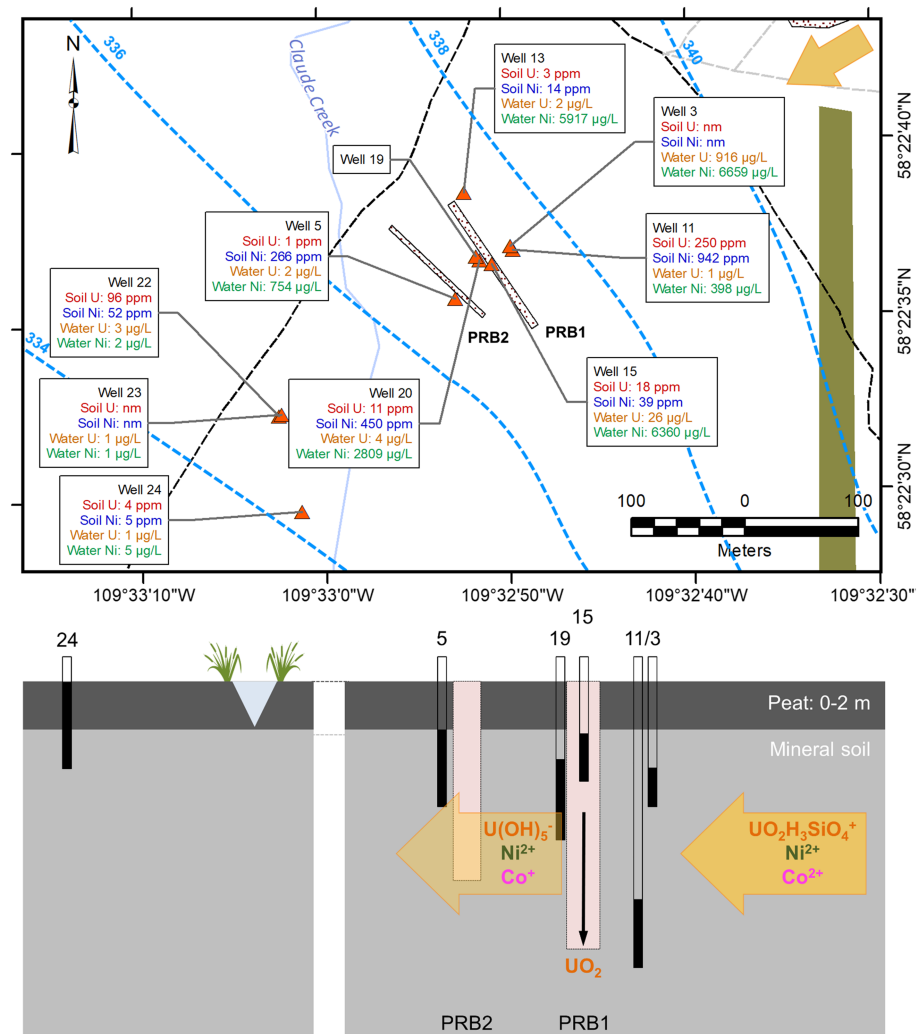


**Figure 1.** (top) Overview map of the sampling locations. In the map, values for U and Ni represent groundwater and soil concentrations and outlines of the PRB2 (southwest) and the PRB1 (northeast) are drawn as textured rectangles between well 5 (downgradient) and wells 3/11 (upgradient). General groundwater flow direction is indicated by the arrow in the top right corner. The blue dashed lines indicate the groundwater equipotential lines (data from AREVA, 2013). (bottom) Artistic depiction of a cross section cutting through the PRBs (not too scale). The filled portions of the wells (black) indicate the approximate extent of the well screens. Dominant metal speciation is shown, as obtained by geochemical modeling. PRB = permeable reactive barrier.

To distinguish the concentrations and binding affinities of trace metals in the wetland, a sequential extraction technique based on the Community Bureau of Reference (CBR) method (Quevauviller et al., 1993), with modifications as described in von Gunten et al. (2017), was performed on the 2017 peat, the 2018 mineral soil, and all PRB1 samples. This method allows for the extraction of organic-rich substrates and considered the following four metal fractions: (1) exchangeable/acid soluble (metals weakly adsorbed to the substrate and to carbonates), (2) easily reducible (Fe/Mn oxyhydroxides), (3) oxidizable (metals sorbed/precipitated to organic matter and sulfides), and (4) residual (strongly bound metals). Extractions were performed with 0.5 g of dried (60 °C) samples in 50-mL polypropylene centrifuge tubes (here further referred to as “reaction tubes”). To reduce sample losses during sample transfer between the extractions, 0.45 µm polyvinylidene fluoride (PVDF) filter centrifuge tubes (Thermo Scientific) were used for solution recovery. For this, after each extraction, the suspensions in the reaction tubes were transferred to the centrifuge filter tubes and centrifuged at 2,000 g for 8 min to recover the solution, which was then analyzed for metal concentrations using an Agilent 8800 triple quadrupole inductively coupled plasma–mass spectrometer (ICP-MS). During ICP-MS analyses, He, H<sub>2</sub>, and O<sub>2</sub> were used as collision and reaction gases to remove polyatomic interferences

**Table 1**  
Sampling Depths, pH Values, and Carbon and Nitrogen Data From Surface Peat (S) and Mineral Soil (M) From the Transect Cutting Through the PRBs1

Location	Depth (cm)	Year collected	pH	TN (wt%)	TC (wt%)	TOC (wt%)
11S	20–30	2017	4.10	1.4	44.8	40.2
11M	110–120	2018	4.94	0.0	0.7	0.7
13S	20–30	2017	3.25	0.7	44.3	42.5
15S	20–30	2017	9.72	0.1	6.7	6.1
15D	90–100	2017	-	0.1	6.8	6.2
15M	200–210	2018	8.75	0.4	22.6	21.3
20S	20–30	2017	5.27	0.7	31.3	31.2
20M	190–200	2018	7.31	0.0	0.6	0.6
05S	20–30	2017	4.06	1.0	38.9	33.9
05M	110–120	2018	3.66	0.1	1.4	1.3
22S	20–30	2017	5.93	0.7	15.5	15.0
24S	20–30	2017	5.07	1.4	43.0	40.9
24M	200–210	2018	2.90	0.1	0.7	0.7

Note. Samples 15 were taken from the PRB material. See Figure 1 for spatial distribution of locations. PRB = permeable reactive barrier; TN = total nitrogen; TC = total carbon; TOC = total organic carbon.

(Sakai, 2015). Residual material in the reaction tubes after each extraction step was transferred to the filter tubes with the addition of ultrapure water and centrifuged again. Additional ultrapure water was added to wash the sample for the next extraction step. After flushing, the solids were transferred back into the reaction tube with additions of water and dried at 60 °C prior to the next step. No ashing was performed for the last digestion step; however, an increased amount of 70% nitric acid (10 ml) was used in the digestion to completely digest the peat-rich samples.

## 2.2. Groundwater Samples

In 2017, groundwater from wells was sampled using a MasterFlex E/S portable sampler (Cole-Parmer). The wells were purged (three well volumes, according to Vail, 2013). Water samples were filtered (0.45 μm) and acidified (pH <2) prior to analysis by ICP-MS. For selected samples, chloride, sulfate, and nitrate were measured by colorimetry according to U.S. Environmental Protection Agency (1983). Briefly, using a Gallery Plus discrete photometric analyzer (Thermo Scientific), chloride was determined by adding mercury thiocyanate and ferric ammonium sulfate to measure the formed ferrithiocyanate complex (method 325.2). Sulfate was determined by precipitation of barium sulfate through barium chloride addition using the turbidimetric method (method 375.4). Nitrate was

analyzed by the hydrazine reduction method, in which nitrate is reduced to nitrite, and the latter is then quantified by diazotization with sulfanilamide and coupling to *N*-(1-naphthyl)-ethylenediamine dihydrochloride (method 353.1).

In 2018, selected wells were similarly purged, and physical/chemical parameters were then recorded on site using an YSI Professional multimeter submerged in a bucket filled with fresh sample from the well. Samples filtered through 0.45-μm membranes were collected for AF4 linked to an ICP-MS (AF4-ICP-MS), which was done to analyze the distribution of trace metals in different colloid types. This method is documented to differentiate between dissolved species, species bound to dissolved organic carbon (DOM), and those bound to inorganic colloids (mainly clays and oxyhydroxides; Cuss et al., 2017). In order to sample anaerobically, inline-filtered water was pumped directly into a glove bag (Fisher Scientific), which was first purged three times with nitrogen gas. Water samples were collected in duplicate, filled into acid-washed 150-mL glass serum bottles, and sealed inside of the glove bag with rubber stoppers.

In the laboratory, the samples were stored in a glove box (98% nitrogen, 2% hydrogen) prior to analysis by AF4-ICP-MS. To prevent oxidation during the measurements, glass autosampler vials were used (filled in an anaerobic glove box), and the instrument eluent was bubbled with Ar for 72 hr before analyses. Ultrapure water and HCl were used to adjust pH and conductivity of the carrier fluid buffer (ammonium carbonate) to the sample properties. The method is described in full detail in Cuss et al. (2017).

In addition to the AF4 samples, to investigate the size distribution of colloidal particles in groundwater, water pumped from the wells was instantly filtered using inline 1.2-, 0.45-, and 0.2-μm high-turbidity filters (Waterra) and ultrafiltration cartridges (Pellicon XL, Millipore, 500 and 10 kDa), both fed with the 0.2-μm permeate. All permeate samples were analyzed for metals and metalloids using the ICP-MS.

## 2.3. Geochemical modeling

Geochemical modeling was performed with PHREEQC V. 3.4.0.12927 and the Minteq.v4 (Parkhurst & Appelo, 2013) database to model the conditions found in the groundwater upgradient and at PRB1. Elemental concentrations were taken to be those measured in upgradient well 3 (Table S2). To simulate the percolation of this water through the PRB, we applied a “forward” modeling approach. The pH was adjusted based on geochemical conditions in well 15 (Table 1), which is located within PRB1 (Figure S1). Temperature was adjusted as measured in wells 3 and 15 (5.5 °C) and the redox conditions ( $p_e$ ) were set based on oxygen concentrations (Table 2). No absolute S(-II) and Fe (II) values were measured; rather, the oxidation states of redox-active elements were calculated by the model (at the modeled  $p_e$  value), which likely does not represent the actual situation in the field but is rather a qualitative approximation. Alkalinity



**Table 2**  
Metal and S Concentrations (ICP-MS Data) and Chemical Parameters Measured in Groundwater as Determined With June 2017 Samples

Site	Depth (m)	Water level (m)	Ca (ppm)	Mg (ppm)	S (ppm)	Mn (ppm)	Fe (ppm)	Co (ppm)	Ni (ppm)	Cu (ppm)	Zn (ppm)	U (ppm)	O <sub>2</sub> (ppm)	Cond (μS/cm)	pH
03	5.0	0.38	257	475	1079	14.9	6.6	1.898	6.659	0.073	1.049	0.916	0.2	2,837	4.6
11	11.8	0.47	394	292	878	4.7	12.2	0.110	0.398	0.002	0.050	<0.001	—	3,472	6.4
13	3.1	0.81	191	441	918	15.7	2.3	1.864	5.917	0.003	1.169	0.002	—	2,651	4.9
15	4.4	0.22	184	450	951	11.7	0.4	1.409	6.360	0.002	0.015	0.026	0.1	2,895	6.0
19	5.8	0.27	210	417	969	12.9	1.4	1.798	6.544	<0.001	0.535	0.171	0.2	3,320	5.3
20	10.1	0.38	332	360	936	11.9	15.5	0.812	2.809	0.004	0.338	0.004	—	3,784	5.7
05	5.0	0.46	212	374	829	6.9	3.8	0.195	0.754	0.003	0.048	0.002	0.2	3,259	6.7
22	1.6	0.69	10	4	3	0.1	10.6	0.001	0.001	0.003	0.011	0.003	—	122	6.3
23	6.8	0.60	32	9	21	0.8	7.2	<0.001	0.001	0.001	0.009	0.001	—	227	6.3
24	5.2	0.05	116	96	277	2.3	17.3	0.001	0.005	0.001	0.016	0.001	4.3	1,404	6.1
Removal efficiency (formula: 1 – concentration in 5/concentration in 3)					18%	21%	23%	54%	42%	90%	89%	96%	95%	100%	

Note. Well 19 data and oxygen concentrations from June 2018. Water level given as meters below surface (June 2017 sampling). Additional well information can be found in Table S5. Removal efficiency was calculated by comparing data from well 3 (upgradient) and well 5 (downgradient). Mo was <0.001 ppm except for groundwater samples 03 and 22 (0.001 ppm). The detection limit for dissolved oxygen was 0.1 ppm. ICP-MS = inductively coupled plasma–mass spectrometer; Cond = specific conductivity.

was estimated based on total inorganic carbon concentrations measured for June 2017 samples using a Shimadzu TOC-V CHN. Given the high solubility of lime, it was assumed to be the only source of alkalinity for PRB1. To account for this, the corresponding simulations included calcite as an equilibrium phase. For reduced scenarios, a  $p_e$  of  $-3$  was chosen based on the highest  $p_e$  values generally found for sulfur-reducing environments (Libes, 2013). Upgradient simulation results were compared with simulations done with PRB1 input values (well 15) under oxic and anoxic conditions (Table S2).

#### 2.4. Stable Isotopes of Water

To investigate groundwater-surface water interactions, we investigated the  $\delta^2\text{H}$  and  $\delta^{18}\text{O}$  isotopic composition in rain water, groundwater from several wells in the wetland and its surroundings, and surface water from creeks and lakes (for locations, see Table S1). Water samples were collected in June and September 2017 and June 2018 using a MasterFlex E/S portable sampler (see above). Samples were then filtered (0.45  $\mu\text{m}$ ) and then analyzed for  $\delta^2\text{H}$  and  $\delta^{18}\text{O}$  values (delta notations, relative to the Vienna Standard Mean Ocean Water, VSMOW) using the Picarro cavity ring-down spectroscopy L2130-i isotopic water analyzer at the UofA with analytical uncertainties of 0.2‰ and 0.6‰ for  $\delta^{18}\text{O}$  and  $\delta^2\text{H}$ , respectively. In addition, water samples were analyzed for their chemical composition using the ICP-MS (Table S1).

#### 2.5. 16S-rRNA gene sequencing

To better understand the biogeochemical conditions in the investigated environment and the potential impact of the waste stream on microbes, DNA was extracted from peat (2017) and mineral soil (2018) samples from the field. DNA was isolated using the FastDNA SPIN Kit for soil (MP Biomedicals), and 16S rRNA was amplified by polymerase chain reaction following the 16S Metagenomic Sequencing Library Preparation Guide by Illumina (2016) and using the universal bacterial and archaeal primers F515 (5'-GTGCCAGCMGCCGCGTAA-3') and R806 (5'-GGACTACHVGGGTWTCTAAT-3'; von Gunten et al., 2018). Sequencing was performed on an Illumina MiSeq platform for pair-end reads using the Illumina NexteraXT library preparation kit. Obtained data were processed using the MetaAmp version 2.0 pipeline (Dong et al., 2017). The amplicons were trimmed to a length of 250 base pairs with a minimum length overlap of 50 base pairs (no mismatches in overlap), and no mismatches were allowed for the primer sequences. Reference alignments were done to the SILVA version 123 database (Yilmaz et al., 2014). Operational taxonomic unit (OTU) clustering was performed at 99% similarity level (Edgar, 2018), and singletons, unknowns, and eukaryotic sequences were removed. R version 3.4.1 and the PHYLOSEQ package were used to plot the community composition (McMurdie & Holmes, 2013; R Core Team, 2017). The distribution of predicted metabolisms was estimated with the METAGENassist tool by Arndt et al. (2012). Selected OTU sequences were aligned with the National Center for Biotechnology Information (NCBI) database using BLAST

(Altschul et al., 1990). Raw sequence reads were submitted to the NCBI database under the bioproject accession number PRJNA513194.

### 3. Results

#### 3.1. Mineralogy

Sieving of the PRB1 material (15S) indicated that the soil particles comprised the following size fractions: >2 mm (83%), 2–1 mm (5%), 1–0.075 mm (11%), and <0.075 mm (1%). Therefore, the sieving supports the reported dominance of the gravel-sized fraction (AREVA, 2013). The pH of this top PRB1 material was between 8.95 and 9.72, which is relatively high compared to that of the groundwater flowing through the PRB1 (pH 6, Table 1), indicating strongly alkaline conditions.

XRD analyses on the soils collected in close proximity to the groundwater wells 11, 20, 5, and 24 (Figure 1) indicated the presence of quartz ( $\text{SiO}_2$ ), microcline ( $\text{KAlSi}_3\text{O}_8$ ), clinocllore ( $(\text{Mg}_5\text{Al})(\text{AlSi}_3\text{O}_{10})(\text{OH})_8$ ), and muscovite ( $\text{K}(\text{Al}_{2.9}\text{Si}_{3.1}\text{O}_{10})(\text{OH})_2$ ) (see Figures S6–S12 for XRD spectra). Traces of pyrite ( $\text{FeS}_2$ ) were found in sample 5M, downgradient of both PRBs. XRD on the PRB1 samples (15S, 15D, and 15M) indicated the presence of quartz, natrolite ( $\text{K}_{14.93}(\text{Al}_2\text{Si}_3\text{O}_{10})_8$ ), microcline, dolomite ( $\text{CaMg}(\text{CO}_3)_2$ ), calcite ( $\text{Ca}(\text{CO}_3)$ ), weddellite ( $\text{CaC}_2\text{O}_4 \cdot 2\text{H}_2\text{O}$ ), kaolinite ( $\text{Al}_2\text{Si}_2\text{O}_5(\text{OH})_4$ ), muscovite, and clinocllore. Further, the following phosphate, sulfate, and sulfide minerals were found: millisite ( $(\text{Na,K})\text{CaAl}_6(\text{PO}_4)_4(\text{OH})_9 \cdot 3\text{H}_2\text{O}$ ), bassanite ( $\text{Ca}(\text{SO}_4) \cdot 0.5\text{H}_2\text{O}$ ), and pyrite.

#### 3.2. Solid Metal Speciation

Upgradient of the PRBs (location 11 or 3), the soil generally contained higher concentrations of metals, as could be expected due to contaminated groundwater (Figure 2). Higher contamination was observed in the peat (20–30 cm) than in the mineral soil (90–100cm). Nickel, for example, had a concentration of 910 ppm in the peat at the surface upgradient of the PRBs (Figure 2) and only 16 ppm in the underlying mineral soil. At PRB1, metal concentrations were generally lower than those in the surrounding peat (with the exceptions of Fe and Mn), likely a result of the higher density of the PRB1 material that mainly consisted of gravel. In the less dense peat material, sorbed and precipitated metals are contributing more significantly to a weight change than in the heavier gravel matrix. An exception was the distribution for Cu, which was more concentrated in the deep PRB samples and all samples downgradient of them. Although most samples downgradient of PRB1 were generally less concentrated in metals than were the upgradient samples (location 11), the isolated location 24 had higher concentrations of many metals in the mineral soil.

Sequential extractions revealed a high abundance of metals in the oxidizable fraction of the peat and the mineral soil below (Figure 2). According to Tessier et al. (1979), this fraction includes organic matter and certain easily oxidizable sulfides. More than 70% of total Ni, Cu, and U were bound to this fraction in the surface peat. The average abundance of all trace elements in this fraction was 57% in peat and only 30% in mineral soil, likely due to the lower organic matter content of the latter. Nickel and Co had similar distributions. In the peat samples, the first two soil fractions (exchangeable/acid soluble and reducing) together comprised on average 25% for Ni and 51% for Co. In the mineral soil, these two fractions represented 84% for Ni and 84% for Co, indicating relatively weaker binding of these metals. This distribution suggests high potential mobility of Ni and Co, as would be expected given that metals in the first two fractions are easily released from the solid phase into the aqueous phase (Yuan et al., 2011). Copper, on the other hand, was mainly present in the more recalcitrant oxidizable and residual fractions, which made together on average 95% in peat and 86% in mineral soil. This was similar to U, which on average was mostly present in the oxidizable and residual fractions (97% in peat and 71% in mineral soil).

In the PRB1 samples, many elements (e.g., Ni, Co, and Cu) showed high recalcitrance with up to 100% of those metals being bound to the two more stable fractions (oxidizable and residual). For U, the more mobile exchangeable/acid soluble fraction made up to 61%, suggesting the presence of uranyl carbonates and uranyl hydroxides. Like U, sulfur (on average 75% exchangeable/acid soluble) was also mobile, likely due to highly soluble sulfates such as bassanite. Being mostly in the first fraction, U and S would be susceptible to changes in ionic strength and acidity, which could easily remobilize their solids-associated forms (Yuan et al., 2011). Iron, being highly concentrated in the PRB1 samples, had a large residual fraction and was, therefore, likely in the form of crystalline compounds such as pyrite (Poulton & Canfield, 2005; Tessier et al., 1979). Mn had a

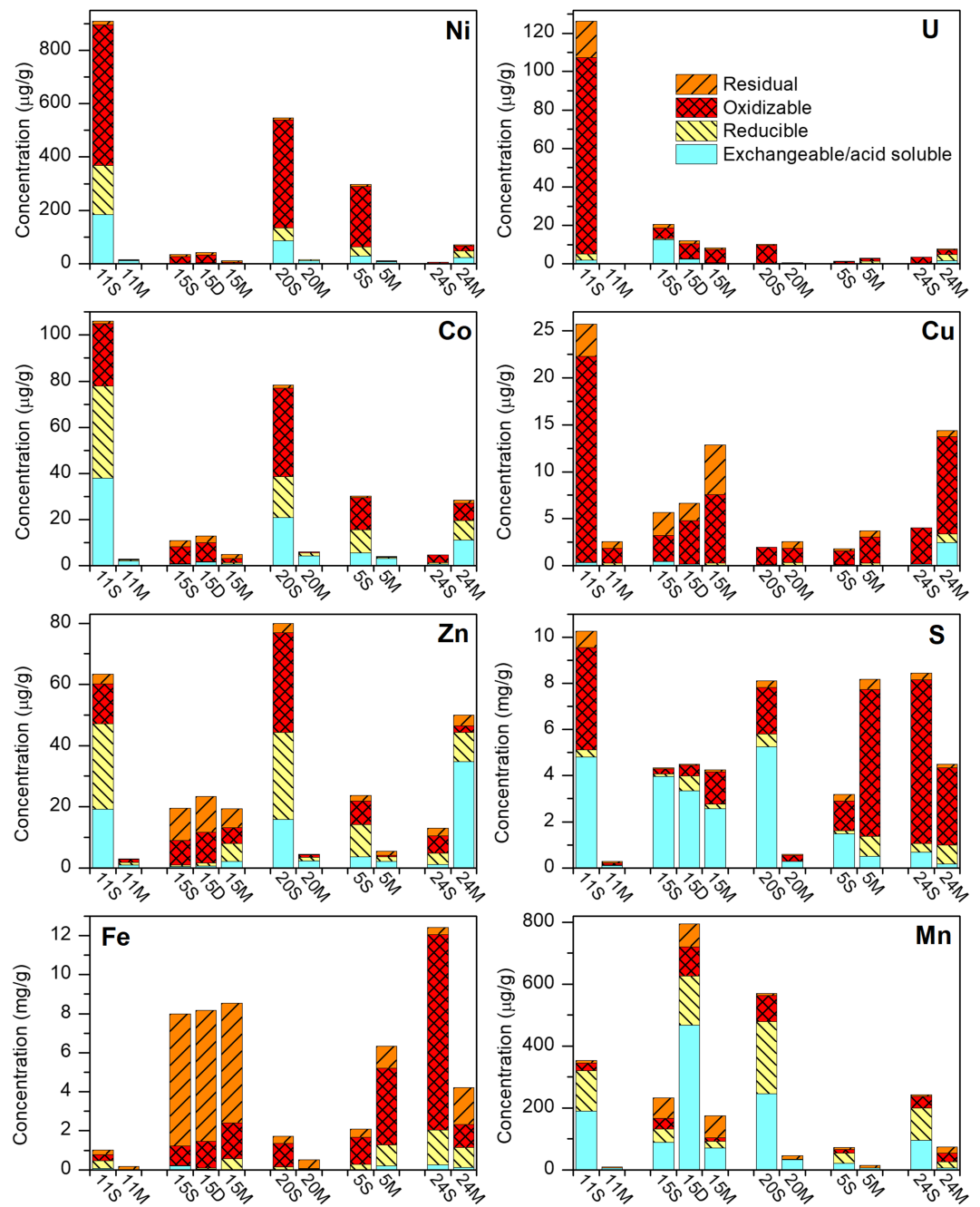


**Figure 2.** Metal distribution over the four solid fractions in peat and PRB samples determined by sequential extraction. For each location, analysis was done on surface peat (“S”) and mineral soil (“M”). For the PRB, 3 samples were analyzed: 20–30 cm (“S”), 90–100 cm (“D”), and 200–210 cm (“M”). PRB = permeable reactive barrier.

significant exchangeable/acid soluble portion (PRB1 average of 63%), suggesting that more mobile Mn forms are accumulated in PRB1. Examples include sorbed  $Mn^{2+}$ , amorphous Mn oxyhydroxides, and rhodochrosite ( $MnCO_3$ ), a mineral that was thermodynamically predicted to precipitate (see the next section and Table 3).

### 3.3. Aqueous Geochemical Trends and Speciation Modeling

Groundwater had elevated metal concentrations at the 5-m-deep upgradient locations (station 3) as compared to similarly deep downgradient sampling points situated in the flow path (e.g., stations 19, 20, and 5;

**Table 3**

Summary of the PHREEQC Modeling Results for Groundwater Based on the Composition Found in Well 3 (Upgradient of PRB1) With Varied pH and  $p_e$  Values

Input source	Upgradient input				PRB1 input			
Conditions	Upgradient pH 4.6, $p_e$ 14.9	PRB, oxic pH 4.6, 14.9, with calcite	pe	PRB, reduced pH 4.6, pe -3.0, with calcite	PRB, oxic pH 6.0, pe 11.4	PRB, reduced pH 6.0, pe -3.0		
Equilibrium pH, $p_e$								
pH	4.6	7.8		6.7	6.0	6.0		
$p_e$	14.9	8.9		-4.8	11.4	-3.0		
Aqueous species (major species and abundance in %)								
Mn	Mn <sup>2+</sup>	74 Mn <sup>2+</sup>	74	Mn <sup>2+</sup>	97 Mn <sup>2+</sup>	74	Mn <sup>2+</sup>	100
Fe	Fe(OH) <sub>2</sub> <sup>+</sup>	99 Fe(OH) <sub>2</sub> <sup>+</sup>	93	Fe(HS) <sub>3</sub> <sup>-</sup>	50 Fe(OH) <sub>2</sub> <sup>+</sup>	100	Fe(HS) <sub>2</sub> <sup>0</sup>	83
Co	Co <sup>2+</sup>	71 Co <sup>2+</sup>	69	Co <sup>2+</sup>	92 Co <sup>2+</sup>	70	Co <sup>2+</sup>	100
Ni	Ni <sup>2+</sup>	61 Ni <sup>2+</sup>	58	Ni <sup>2+</sup>	83 Ni <sup>2+</sup>	62	Ni <sup>2+</sup>	100
Cu	Cu <sup>2+</sup>	60 CuCO <sub>3</sub> <sup>0</sup>	70	Cu(S <sub>4</sub> ) <sub>2</sub> <sup>-3</sup>	72 Cu <sup>2+</sup>	60	Cu(HS) <sub>3</sub> <sup>-</sup>	98
Zn	Zn <sup>2+</sup>	52 Zn <sup>2+</sup>	50	Zn(HS) <sub>3</sub> <sup>-</sup>	68 Zn <sup>2+</sup>	53	Zn(HS) <sub>3</sub> <sup>-</sup>	61
U	UO <sub>2</sub> H <sub>3</sub> SiO <sub>4</sub> <sup>+</sup>	63 UO <sub>2</sub> (CO <sub>3</sub> ) <sub>3</sub> <sup>-4</sup>	96	U(OH) <sub>5</sub> <sup>-</sup>	99 UO <sub>2</sub> SO <sub>4</sub> <sup>0</sup>	42	U(OH) <sub>5</sub> <sup>-</sup>	95
S	SO <sub>4</sub> <sup>2-</sup>	68 SO <sub>4</sub> <sup>2-</sup>	68	H <sub>2</sub> S	71 SO <sub>4</sub> <sup>2-</sup>	70	H <sub>2</sub> S	94
Potential precipitates (saturation indices)								
Dolomite	CaMg(CO <sub>3</sub> ) <sub>2</sub>	Not predicted	<b>0.3</b>	<b>0.0</b>	-7.4	-7.0		
Gypsum	CaSO <sub>4</sub> ·2H <sub>2</sub> O	-0.2	-0.1	-11.0	-0.4	-5.3		
Kaolinite	Al <sub>2</sub> Si <sub>2</sub> O <sub>5</sub> (OH) <sub>4</sub>	<b>4.9</b>	<b>14.0</b>	<b>13.8</b>	<b>7.1</b>	<b>7.4</b>		
Birnessite	MnO <sub>2</sub>	-1.0	-1.0	-31.3	-2.3	-30.9		
MnS	MnS	-128.0	-102.0	-0.1	-111.8	-1.5		
Rhodochrosite	MnCO <sub>3</sub>	Not predicted	<b>0.6</b>	<b>0.3</b>	-3.2	-3.0		
Ferrihydrite	Fe(OH) <sub>3</sub>	<b>1.1</b>	<b>4.3</b>	-11.0	<b>1.2</b>	-11.2		
Magnesioferrite	Fe <sub>2</sub> MgO <sub>4</sub>	-3.2	<b>9.8</b>	-22.6	<b>0.1</b>	-24.5		
Magnetite	Fe <sub>3</sub> O <sub>4</sub>	<b>3.6</b>	<b>16.4</b>	-15.0	<b>6.2</b>	-16.6		
Goethite	FeOOH	<b>3.9</b>	<b>7.1</b>	-8.1	<b>4.1</b>	-8.3		
Mackinawite	FeS	-129.4	-103.6	-0.7	-113.8	-1.8		
Pyrite	FeS <sub>2</sub>	-207.3	-168.6	<b>10.1</b>	-182.3	<b>10.9</b>		
Na-Jarosite	NaFe <sub>3</sub> (SO <sub>4</sub> ) <sub>2</sub> (OH) <sub>6</sub>	<b>4.5</b>	<b>4.4</b>	-60.6	<b>0.8</b>	-46.8		
Co(OH) <sub>3</sub>	Co(OH) <sub>3</sub>	-7.9	-4.6	-20.8	-7.1	-21.3		
CoFe <sub>2</sub> O <sub>4</sub>	CoFe <sub>2</sub> O <sub>4</sub>	<b>15.8</b>	<b>28.7</b>	-3.8	<b>18.9</b>	-5.6		
CoS(α)	CoS	-120.9	-95.1	<b>6.9</b>	-104.7	<b>5.5</b>		
Ni(OH) <sub>2</sub>	Ni(OH) <sub>2</sub>	-9.4	-2.9	-4.9	-6.5	-6.3		
NiS(α)	NiS	-122.1	-96.3	<b>5.7</b>	-105.8	<b>4.5</b>		
Cu(OH) <sub>2</sub>	Cu(OH) <sub>2</sub>	-6.8	-1.0	-22.2	-5.5	-22.4		
Chalcocite	Cu <sub>2</sub> S	-123.8	-86.3	<b>3.6</b>	-103.8	<b>1.2</b>		
Antlerite	Cu <sub>3</sub> (OH) <sub>4</sub> SO <sub>4</sub>	-12.2	-1.2	-74.1	-11.4	-67.2		
Cupricferrite	CuFe <sub>2</sub> O <sub>4</sub>	<b>4.3</b>	<b>16.5</b>	-35.1	<b>5.9</b>	-35.8		
Cuprousferrite	CuFeO <sub>2</sub>	-0.4	<b>11.9</b>	-10.4	<b>3.1</b>	-11.8		
Chalcopyrite	CuFeS <sub>2</sub>	-225.7	-174.7	<b>11.1</b>	-195.3	<b>9.8</b>		
Covellite	CuS	-106.2	-81.0	<b>1.8</b>	-104.7	<b>1.6</b>		
Zn(OH) <sub>2</sub>	Zn(OH) <sub>2</sub>	-8.5	-2.1	-13.4	-7.5	-14.7		
Zn <sub>4</sub> (OH) <sub>6</sub> SO <sub>4</sub>	Zn <sub>4</sub> (OH) <sub>6</sub> SO <sub>4</sub>	-24.9	-5.6	-60.1	-23.6	-57.7		
ZnS(am)	ZnS	-119.4	-93.6	-0.9	-104.9	-2.1		
UO <sub>2</sub> (am)	UO <sub>2</sub>	-28.0	-21.0	<b>0.0</b>	-22.3	-0.8		
Uraninite	UO <sub>2</sub>	-22.0	-15.0	<b>6.0</b>	-16.3	<b>5.2</b>		
UO <sub>2</sub> (OH) <sub>2</sub> (β)	UO <sub>2</sub> (OH) <sub>2</sub>	-4.1	-3.6	-11.0	-2.5	-9.9		

Note. As a comparison, modeling results based on the composition in well 15 (PRB1) are shown. Where calcite was added as an equilibrium phase, pH and  $p_e$  were allowed to equilibrate and are given in the top rows. In the solids section below, saturation indices are positive (bold) for species that are expected to precipitate. am = amorphous; PRB = permeable reactive barrier.

Table 2). Groundwater from the deeper wells had generally lower metals concentrations; for example, in well 3, Ni and U were 6,660 and 916 ppb, respectively, compared to 398 and <1 ppb, respectively, in well 11 (Figure 1). At the PRB1 (location 15) the groundwater did not show elevated Ca concentrations as would be expected due to the presence of lime and limestone; it was, however, still enriched in U (26 ppb), Ni (6,360 ppb), and Co (1,410 ppb). Downgradient of the two PRBs (site 5), groundwater had lower concentrations of most elements, with the exception of S (829 ppm). The overall removal efficiencies in groundwater for transition metals and U were >43%, with U, Cu, and Zn having the highest values



(Table 2). It should be noted that these removal efficiencies were calculated based on the current situation (e.g., 10–11 years after PRB1 installation) and with the assumption that the sampled monitoring wells are situated along the direction of groundwater flow.

The specific conductivity (Table 2) was elevated in all wells in proximity of the PRBs and also at the isolated location 24 (Figure 1), suggesting that a fraction of the waste plume could be passing underneath or around the PRB. The first option is supported by elevated concentrations for Fe and Mn found in the 10-m-deep well 20 between the two PRBs (Table 2). The second option is supported by high metal concentrations found in well 13 located on the north end of the PRB1. In any case, the circumvention of the PRBs by groundwater could explain the high metal concentrations in well 24 (e.g., 17 ppm for Fe) which is located about 240 m downgradient of the PRBs. Dissolved oxygen values measured in June 2018 varied from 0.1 to 0.2 ppm in the surrounding of the PRBs, suggesting a low-oxygen environment. At the same time, no nitrate-N could be detected in wells 15 and 20. Sulfate-S (determined by colorimetry), however, was high for the tested wells 15 and 20 with concentrations of 1,080 and 1,030 ppm, respectively. Assuming that Fe and Mn were in their mobile 2+ oxidation state, the high abundance of sulfate would allow for the formation of a sulfate-reducing environment. This was confirmed by the strong hydrogen sulfide smell of disturbed peat and mineral soil samples in the field, indicating active sulfur reduction.

Geochemical modeling that uses the measured oxygen concentrations in well 3 (upgradient of PRBs, Figure 1) suggests that in the groundwater flowing southwest, divalent transition metal species would dominate (e.g.,  $\text{Mn}^{2+}$ ,  $\text{Co}^{2+}$ , and  $\text{Ni}^{2+}$ ), while Fe and U are expected to be in their oxidized forms, for example,  $\text{Fe}(\text{OH})_2^+$  and  $\text{UO}_2\text{H}_3\text{SiO}_4^+$  (Table 3, summary in Figure 1). This model does not consider interactions with organic matter. In reality, many processes might cause deviations in the speciation of Fe; for example, Fe (III) could be reduced by organic matter (Lovley & Phillips, 1986), which would explain its mobility in the system. On the other hand, complexation of Fe (III) by organic ligands would allow it to stay mobile even under oxic conditions. When this water reaches PRB1 at oxidizing conditions, the water in contact with limestone would reach an equilibrium pH of 7.8 and an equilibrium  $p_e$  of 8.9, conditions at which Fe, Cu, and U would more readily form complexed species, for example,  $\text{Fe}(\text{OH})_2^+$ ,  $\text{CuCO}_3^0$ , and  $\text{UO}_2(\text{CO}_3)_3^{-4}$  (Table 3). The  $\text{O}_2$  measurements were, however, close to the detection limit of the instrument, and the distinct smell of sulfide suggested anaerobic conditions in the groundwater. When taking this into account and using a  $p_e$  of  $-3.0$  (Table 3, middle column), the equilibrium pH would change to 6.7 and the  $p_e$  would stay reducing at  $-4.8$ . Apart from Mn, Co, Ni (free ions), and U (hydroxide), most metals would start forming sulfide complexes such as  $\text{Fe}(\text{HS})_3^-$  and  $\text{Zn}(\text{HS})_3^-$ . These conditions were compared to modeling results that used actual PRB1 chemical data (well 15) as input under oxic and anoxic conditions ( $p_e$  11.4 versus  $-3.0$ ). Under anaerobic conditions, these results are comparable to the flow-through scenario that used well 3 as input data, yielding both a similar equilibrium pH and similar metal speciation.

Precipitating species, predicted based on their saturation indices (Table 3, lower part), indicate that under oxic conditions no Ni solid phases and a limited number of Co-containing phases (e.g.,  $\text{CoFe}_2\text{O}_4$ ) would form. Under anoxic conditions sulfide species (e.g., CuS,  $\text{Cu}_2\text{S}$ , CoS, and NiS) and uraninite ( $\text{UO}_2$ ) have the potential to precipitate. Those conditions would also favor the formation of pyrite and potentially dolomite, minerals identified by XRD analysis (see above).

### 3.4. Water Isotopic Data

Using  $\delta^{18}\text{O}$  and  $\delta^2\text{H}$  data obtained from rain water, groundwater, and surface water, the local evaporation line was constructed, yielding the following equation:  $\delta^2\text{H} = 4.88 \delta^{18}\text{O} - 57.8$  (Figure S2). The local evaporation line slope is typical of those for high latitudes (Gibson et al., 2016). The June 2017 values plot in the lighter region, indicating that evaporation left behind heavier water in September 2017. The local meteoric water line was obtained by plotting a fit through the rain water samples and samples measured from the deeper wells that did not show large variation between June and September. The latter group of samples turned out to be from the investigated wetland, suggesting that those wells did not experience enrichment of heavier isotopes by evaporation processes. Thus, groundwater in the wetland likely originated from relatively rapid percolation of precipitation through the waste rock pile located in the northeast (von Gunten, Warchola, et al., 2018). The obtained slope of the local meteoric water line was 7.7, which corresponds to the Saskatchewan average of 7.7 (Pham et al., 2009). Additionally,  $\delta^2\text{H}$  and  $\delta^{18}\text{O}$  of surface water collected on

top of both PRBs was similar to groundwater from the wetland wells (see Table S1 for details), suggesting that this water is strongly influenced by groundwater and is not simply accumulated rain water.

### 3.5. Colloidal Metal Distribution

AF4-ICP-MS analyses revealed colloid-associated trace metals in the 0.45- $\mu\text{m}$  filtered water, especially for the transition metals Co, Ni, and Cu and the heavier elements Pb, Th, and U (Figure 3). Cobalt and Ni were strongly associated with the DOM fraction at PRB1 (well 15) and in the isolated well 24 beyond the creek. Both have relatively high water pH levels (approximately pH 6), and this suggests complexation with organic acids (i.e., humic acids). Compared to Co and Ni, Cu showed an even stronger association with DOM and also with inorganic colloids, especially at well 15 and also in the downgradient locations (wells 19, 5, and 24). Judging by the low abundance of colloidal Fe and Mn, the inorganic particles likely consisted of clay particles. The following metals dominated the free ionic species: Ca, Mg (data not shown), Mn, Mo, Zn, and As. Increased acidity of the deep upgradient well 3 water (pH 4.6) favored free ionic species for the majority of the metals, with exceptions of Al, Th, and U. Uranium is known to form strong complexes with humic acids even at low pH values in both common oxidation states: U (IV) and U (VI) (Li et al., 1980).

Sequential filtration results (Figure S3) confirmed the AF4-ICP-MS findings that indicate Ni and Co express similar colloidal distributions. In the upgradient water (well 3), clear differences in concentrations were not found for all size fractions, suggesting that the majority of Ni and Co was in the dissolved form (<10 kDa). Water from well 19 (between both PRBs) contained large particles (>1.2  $\mu\text{m}$ ) that carried substantial amounts of Mn, Fe, Ni, Co, Zn, As, and Al. These particles were likely well sediments disturbed by pumping. Filtration results for TOC suggest that the observed DOM particles mentioned above were mostly low molecular weight, that is, <10 kDa for the wells 3 and 19 (i.e., upgradient and middle). Approximately 75% of the TOC in the groundwater at well 15 (PRB1) was <10 kDa, the rest being up to 200 nm in size, suggesting that the DOM increased in size at PRB1. About 80% of the TOC in the isolated groundwater well 24 was in the 10- to 500-kDa fraction, with the rest being <10 kDa. At PRB1, many elements (e.g., Al, Co, Ni, Cu, Zn, and As) became evident in the colloidal fractions >450 nm, suggesting the formation of larger colloids in the alkaline environment of the reactive medium.

### 3.6. Prokaryotic Community Changes

16S rRNA gene sequencing indicated that all surface peat samples in the proximity of the PRB (11S, 20S, and 5S) had similar microbial communities (Figure S4). These communities were dominated by bacterial classes Alphaproteobacteria and Betaproteobacteria, Acidobacteria, and Sphingobacteriia. The mineral soil samples (i.e., 11M, 20M, 5M, and 24M), in general, showed a higher abundance of the classes Anaerolineae, Deltaproteobacteria, Nitrospira, and, in the case of the locations 11 (upgradient) and 24 (isolated), Methanomicrobia. Many of the dominant OTUs found in the upgradient sample 11S were closely related to fermentative and acidotolerant microbes, such as *Pseudolabrys*, *Ignavibacterium*, *Bryobacter*, *Acidothermus*, and a representative of the Verrucomicrobia phylum (Table S3), many of which were previously found in wetlands (Drake & Horn, 2009; Iino et al., 2010; Juottonen et al., 2017; Kämpfer et al., 2006; Kulichevskaya et al., 2010). At PRB1, the shallow and deep samples (15S and 15M) showed a similar distribution of classes, dominated by Bacteroidia and Clostridia (Figure S4). Compared to the surrounding samples, more OTUs related to alkalitolerant and alkaliphilic microbes were found, such as *Alkalibacterium*, *Chitinispirillum*, *Geosporobacter*, *Proteiniclasticum*, *Desulfatirhabdium*, *Geofilum*, *Erysipelothrix*, *Desulfomicrobium*, *Caldicoprobacter*, and *Draconibacterium* families (Balk et al., 2008; Bouanane-Darenfed et al., 2014; Hong et al., 2015; Miyazaki et al., 2012; Rozanova et al., 1988; Sorokin et al., 2016; Wang & Riley, 2015; Yumoto et al., 2014; Zhang et al., 2010).

Species richness (i.e., Chao1 index) was generally lower in the mineral soil samples (Figure 4), indicating that fewer species were able to become established in the sandy till compared to the overlying peat. The diversity (inverse Shannon index), on the other hand, was relatively similar between peat and corresponding mineral soil samples. PRB1 showed the highest inverse Shannon indices, suggesting that the reactive medium supported a more diverse microbial community. This PRB effect lasted also further downgradient (location 20).

METAGENassist analyses suggested that ammonia oxidizers, sulfide oxidizers, and sulfate reducers were the most represented metabolisms, making 12–19%, 4–16%, and 8–16% of the community, respectively (Figure 4). Redox conditions were likely dominated by sulfur reduction as suggested above, which is

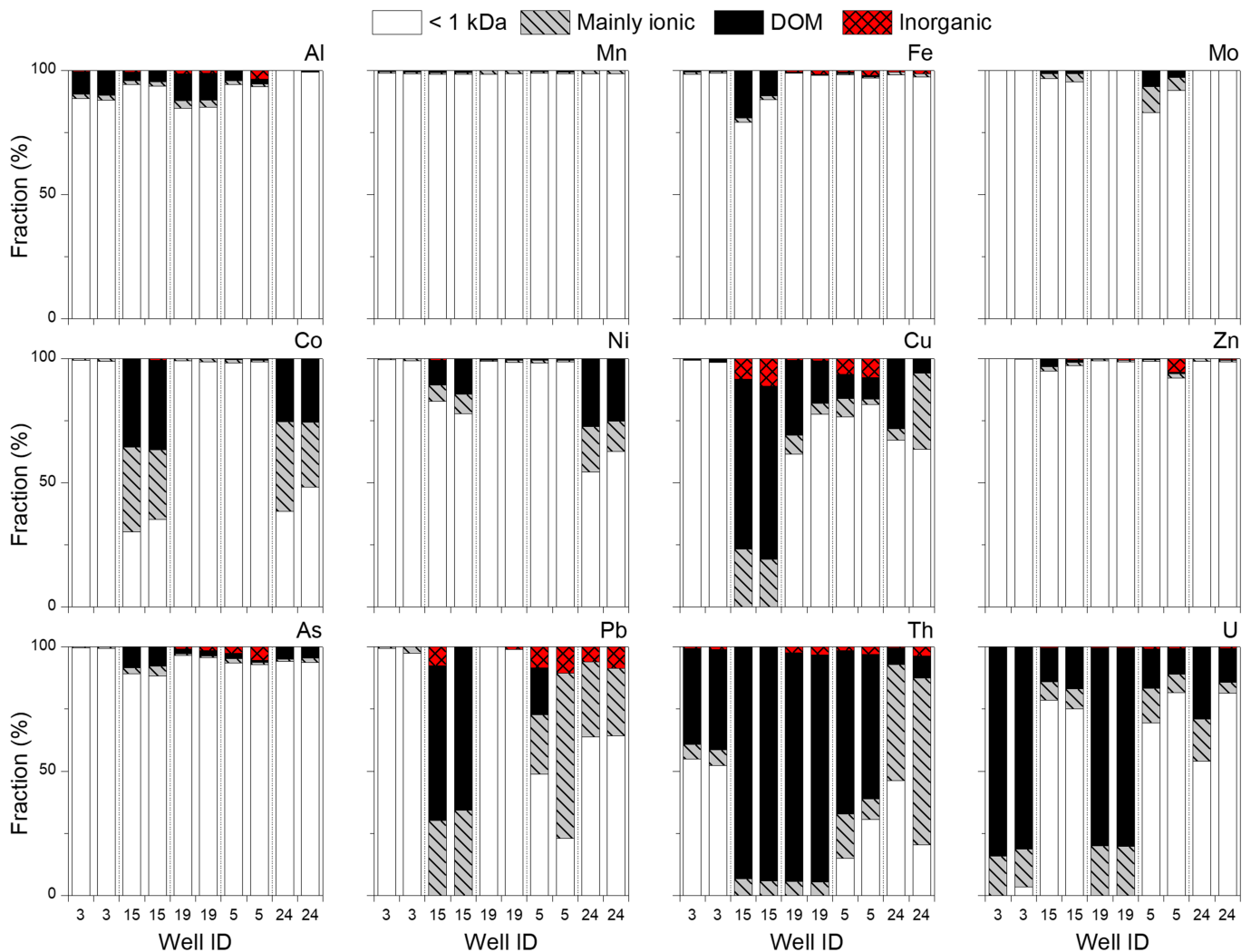


**Figure 3.** AF4-ICP-MS results for selected elements. Each well was measured in duplicates. The first two fractions (<1 kDa and mainly ionic) represent highly mobile proportions of the elements, which are unlikely to be associated with colloids. DOM = dissolved organic matter colloid-associated fraction; Inorganic = fraction associated with inorganic colloids (e.g., aluminosilicates and iron oxides). For well locations, see Figure 1.

typical for non-iron PRBs (Powell et al., 1998). As expected, methanotrophs (overall 0.091–3.684%) were often dominant in the surface-exposed peat layers, whereas methanogens (overall 0.003–1.878%) were more abundant in deeper mineral soil. Given that Co, Ni, Cu, and Zn were highly concentrated in the waste stream and are known to be important cofactors for methanogens and methanotrophs (Glass & Orphan, 2012; Scheller et al., 2010), it was expected that they would enhance the presence of those metabolisms, as was previously demonstrated in laboratory and field studies (Basiliko & Yavitt, 2001; Patel & Sprott, 1990). However, no clear increase of these metabolic groups could be observed in this study. The isolated location 24 and the upgradient location 11 both showed similar abundances of methanogens and methanotrophs. This overall low abundance of methane-related metabolisms could be related to their suppression by sulfate-reducing bacteria (Dise & Verry, 2001; Oude Elferink et al., 1994), although the two metabolic pathways are not mutually exclusive and depend on the rate of sulfate reduction (Sela-Adler et al., 2017).

To test for methanotrophy, surface peat from the locations 5 (downgradient of PRBs) and 11 (upgradient of PRBs) was incubated anaerobically (Figure S5). Methane became detectable after 2 months of incubation. The less contaminated peat from location 5 generated relatively more methane with a lighter  $\delta^{13}\text{C}\text{-CH}_4$  signature (Figure S5), suggesting higher activity of methanogens. This finding was supported by 16S rRNA gene sequencing on those samples, showing 10 times more sequences related to potential methanogens in the

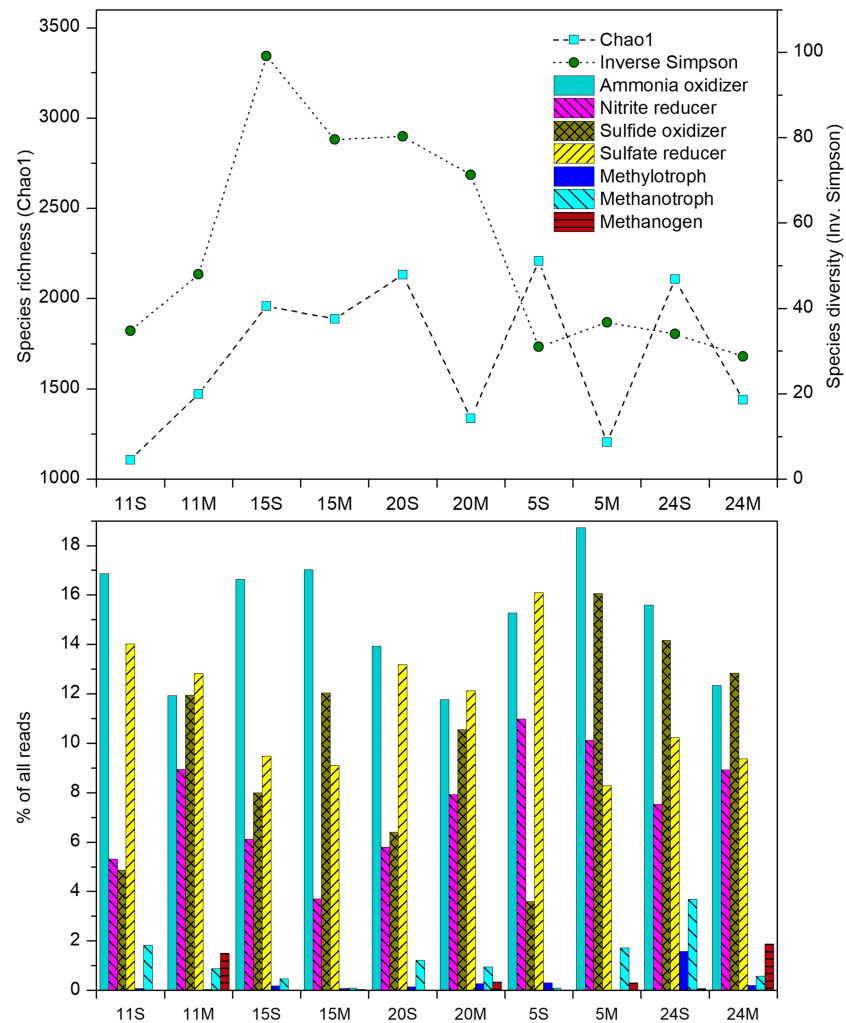


**Figure 4.** Species richness, diversity, and potential metabolisms in the analyzed surface peat (“S”) and mineral soil (“M”) samples.

incubated location 5 sample than in sample 11, without substantial differences in the amount of methanotrophy-related sequences (Figure S5). The major potential methanogen was an archaeon related to *Methanosarcina*, while dominant, presumed methanotrophs were relatives of *Methylocella* and *Methylovirgula*. This test indicated that in the case of the Cluff Lake PRB1, the increased concentrations of transition metals are likely not promoting methanogenesis in the near-surface soil.

Relatives of bacteria being potentially capable of reducing U (VI) were mostly found in the upgradient mineral soil sample 11M, the deep PRB1 sample 15M, and the mineral sample located between the two PRBs, 20M. Examples include *Clostridium* (Gao & Francis, 2008), *Geobacter* and *Shewanella* (Newsome et al., 2014), *Desulfovibrio* (Lovley et al., 1993), and *Desulfosporosinus* (Alessi et al., 2014; Suzuki et al., 2004) with abundances up to 0.051%, 0.150%, 0.005%, 0.309%, and 1.141%, respectively (Table S4). Species of *Desulfosporosinus*, one of the most prominent potential U (VI) reducers, are known to grow autotrophically on hydrogen and sulfate and were found to enzymatically reduce U (VI) under bicarbonate depletion, a condition likely dominant around the PRB1 due to an elevated pH.

## 4. Discussion

### 4.1. Biogeochemical Fate of Metals Passing Through the PRB

Generally, the mobility of Co, Ni, Cu, and Zn in soil and groundwater environments can be ordered as Ni > Co > Zn > Cu (Dean, 1999; Irving & Williams, 1953; Rashid, 1974; Sheoran & Sheoran, 2006), which

indicates that it is generally challenging to immobilize Co and more so Ni. This explains their elevated concentrations in the wetland groundwater at Cluff Lake and their mobility in peat and mineral soil (large exchangeable/acid soluble and reducible fractions).

Given the METAGENassist results that suggest the dominance of sulfate-reducing microbial metabolisms, we expect that the PRB environment is likely anaerobic, which is corroborated by our forward modeling results and by the distinct hydrogen sulfide smell in the field. Modeling suggests that under such reducing conditions precipitation of certain sulfides is favorable, such as pyrite, CoS, NiS, Cu<sub>2</sub>S, and ZnS. Using the modeled equilibrium pH at the time of PRB installation (i.e., pH 9) in the forward model, we predicted that while uraninite is still prone to precipitation and that certain Cu and Zn compounds would be able to form (e.g., Cu<sub>2</sub>S and Zn (OH)<sub>2</sub>), essentially no Ni and Co would precipitate (Table S6). Lower pH generally promotes sulfide formation and therefore transition metal immobilization, which means that the presence of alkaline PRBs may have worsened the situation for Ni and Co immobilization. However, previous investigations (refer to Figure C.17.2 in AREVA, 2013) indicated that the PRBs managed to decrease Ni and Co between 2006 and 2012 from 6 to <1 mg/L downgradient of the PRBs (location 5), which was likely due to metal sorption to the PRB material. The lower efficiency observed today might be an indication that the sorption (e.g., onto organic materials) and precipitation (e.g., as sulfides) capacities of the barriers are exhausted and that the PRBs are nearing the end of their life spans.

In terms of sorption capacity of a PRB, competition reactions with metals can have a detrimental effect on the degree of sorption, particularly for metals such as Ni that bond more weakly than other divalent cations. For example, sorption of Cu can outcompete Ni, due to stronger bond formation (Ho et al., 1996). Copper is especially strongly binding to organic matter (Yang et al., 2015), which explains the large oxidizable fraction determined by sequential extraction and the large colloidal DOM fraction determined by AF4 for Cu. Ni could potentially sorb to microbial biomass under low pH conditions (Zandvoort et al., 2006), but that would depend on the composition of the organic material, that is, the availability of organic ligands that deprotonates at low pH. Although an increase of colloidal TOC at PRB1 (Figure S3) suggests some increase in microbial activity, and Ni (with Co) are indeed partially bound to colloidal DOM particles, the degree of biomass growth is likely insufficient to remove large amounts of Ni, reasons for which are elaborated below in section 4.3.

The observed difference between the solid pH >9 and pH 6 of the groundwater at the PRB (well 15) shows that groundwater does not reside within the PRB for a sufficient time to reach chemical equilibrium or that the easily soluble portion of the alkaline reactive medium has been used up since the installation of the PRBs. Our estimates on groundwater velocities made with water depths measured in June 2017 (Table 2) coupled to station elevations (Table S5) suggest an average Darcy flux of more than 20 cm/day through the PRB. This value is what could be expected in a medium-coarse sandy soil. Note that we used an average hydraulic conductivity of  $1.8 \cdot 10^{-4}$  m/s, estimated with the PRB composition given in section 1 and with literature values by Päivänen (1973) and Domenico and Schwartz (1990).

The high abundance of Fe in the system and the formation of pyrite, and possibly other iron sulfides at the PRB and downgradient of it (e.g., location 5M), has implications for metal removal. This process, which was previously described in PRBs (biobarriers with sulfate reduction; e.g., Herbert et al., 2000), not only reduces the concentration of Fe in the groundwater (Table 2) but could also lead to the sorption and coprecipitation of contaminants onto Fe sulfide phases, for example, As (Saunders et al., 2018) and Cu (Yang et al., 2016). Natrolite, a zeolite detected by XRD, could also contribute to the removal of As and transition metals. Although not a major phase, natrolite could remove metals and metalloids from the aqueous phase through ion exchange and sorption (Interstate Technology and Regulatory Council, 2011).

Uranium, as the major target metal for removal, is efficiently removed by several processes. Under anaerobic conditions, U (VI) can be reduced to U (IV) by Fe (II) species and various Fe (III) and sulfate reducing bacteria. Given the high concentration of Fe, the dominance of reducing conditions and the high abundance of potential sulfate reducing microbes in the Cluff Lake wetland system, these processes are likely to be ongoing and might be responsible for the formation of a dominant oxidizable fraction for U as observed by the sequential extractions. Similarly, Newsome et al. (2014) observed a large oxidizable fraction for U in clay-rich sediments that showed active bioreduction of U (VI). At PRB1, under low-oxygen conditions, U (VI) likely precipitates by forming uranyl carbonates and possibly uranyl hydroxides, such as



paulscherrite, as supported by a large exchangeable/acid soluble soil fraction in the surface sample 15S and by thermodynamic modeling (Table 3).

While the PRBs seems to efficiently remove U, Cu, and Zn, substantial portions of these metals were found to be binding to the solid phase as determined by sequential extractions of upgradient soil. Here many metals including Ni, Co, Mn, and Zn were found to bind to the easily mobilizable exchangeable/acid soluble fraction. This fraction could be remobilized in future in the case of significant changes in ionic strength and acidity of the waste stream (i.e., through acid mine drainage generation). U bound to PRB1 solids could be mobilized in the same manner. Other metals that are more stable in the solid phase (i.e., being in the oxidizable and residual fractions), such as Cu and U, would remain in the peat for longer periods of time but may eventually require remedial actions.

#### 4.2. Formation and Role of Colloidal Particles

Larger ( $>0.45 \mu\text{m}$ ) colloidal particles were found in the groundwater in the first PRB and the groundwater samples taken downgradient of it (e.g., wells 19, 5, and 24). Many DOM and inorganic colloids also emerge in the groundwater after passing through the PRB1 (Figure 3). The colloids are likely formed by the degradation of organic matter (decay of peat and microbial biomass) and the physical breakdown of clays. Taking this into account, major contaminants in water can be divided into four groups: (1) truly dissolved (Mn, Fe, and Zn), (2) partially DOM associated at the PRB and in the isolated well (Ni and Co), (3) DOM associated at  $\text{pH} \geq 6$  (Cu), and (4) mostly DOM associated (U). Thorium, although not a major contaminant, is associated with the latter group as well. The overall small colloidal fractions of Mn, Fe, and Zn is likely related to the pH conditions, as previously shown by thermodynamic modeling. Furthermore, reducing conditions within the peat would favor divalent species of most transition metals and, therefore, increase their mobility. Similar effects play an important role for the second group for Ni and Co; however, the environments within PRB1 and at well 24 (isolated) seem to favor their binding to DOM. For the third group, the previously discussed affinity of Cu to organic matter is responsible for the high abundance of DOM-associated Cu, especially at PRB1. Finally, in the fourth group, U is strongly bound to DOM, except for environments with higher pH values (e.g., PRB1 and isolated location), suggesting that the formation of carbonates is the controlling factor. Thorium, being an actinide such as U, behaves similarly, although it does not show as strong changes to pH as U (Figure 3). It also has a greater DOM-associated fraction, likely due to its inability to be easily oxidized from its major oxidation state Th (IV) (Adams et al., 1959) and due to its high affinity to organic ligands (Langmuir & Herman, 1980).

Metals that exhibit stronger affinity to the solid phase consequently also form more colloid-associated fractions. For example, the average colloidal fraction of Fe is higher (4%) than that of Mn ( $<1\%$ ), and Fe is more strongly bound to the solid phase (88% oxidizable and residual versus 37% for Mn). Copper and U that have high removal rates in groundwater (Table 2) are more represented in the colloidal phase for all groundwater samples (on average 28% and 43%, respectively) and are bound to more recalcitrant solid phase fractions (oxidizable and residual: 88.4% and 72.5%, respectively). On the other hand, Co and Ni both have lower removal rates, have a small colloidal fraction (on average 13% and 8%, respectively), and are relatively mobile (oxidizable and residual: 30% and 31%, respectively). These results suggest that colloidal particles scavenge metals from the groundwater and promote removal processes. In the case of U, this is different than the observations of Wang et al. (2013) and Graham et al. (2011) for wetland and clay-loam soil pore water and groundwater, where colloidal particles contributed to a higher mobility of U. Contrary to these studies, Tran et al. (2018) observed that in a carbonate-rich environment, U (and Cs) was more mobile as dissolved species than as colloid-associated forms. Therefore, the conditions of the PRBs at Cluff Lake could favor the binding of actinides (U and Th) and the transition metals (Cu and Zn) to colloids, which would promote their immobilization (i.e., through colloidal pumping; Honeyman & Santschi, 1991). By contrast, there seems to be a limited effect on Ni, Co, Mn, and Fe, due to their prevalence in the free ionic form. However, it is important to mention that we analyzed groundwater collected from wells for colloidal fractions, which could be altered due to interaction with the filter pack material. While it was not possible for us to obtain sufficient amounts of pore water at the site, future studies should consider the installation of pore water collection devices (e.g., use of multichamber piezometers similar to that in Wang et al., 2013) to sample colloids in a more direct way.

### 4.3. Further Considerations and Potential Improvement Possibilities

Divalent metals can be removed from wetlands either under aerobic conditions by sorption or under anaerobic conditions by sulfate reduction. In an experiment by Eger (1994), the first method was shown to efficiently remove Ni, provided the water level on the surface was not in excess of 5 cm to allow sufficient contact between air and the peat. At our field site, other than the creek flowing through the wetland, no additional surface water flow is documented, although the older 2006 PRB was observed to develop substantial amounts of standing water on top (likely groundwater seepage as indicated by water isotopes), while PRB1 showed some puddles on the surface (Figure S1). According to Eger (1994), an efficient treatment under anaerobic conditions would require (1) the establishment of anoxia at the treatment zone, (2) sufficient amounts of bioavailable sulfate, and (3) an easily degradable substrate that would increase the activity of sulfate reducing bacteria. By using the metal concentrations and pH conditions found in well 3 upgradient of the PRBs, and using the formula by Eger (1994), one can estimate the total requirement of sulfate, assuming that all Al and Fe is in the trivalent form and considering divalent metal concentrations of Mn, Co, Ni, Cu, and Zn. This approach yields 0.014 M of sulfate required, half the concentration of seawater but more than 10 times higher than that in surrounding freshwater (e.g., Cluff Lake as reported by von Gunten, Warchola, et al., 2018), except for mining sites (e.g., up to 0.052 M in Benner et al., 1999). In the case of well 3, the water contains approximately 0.034 M of  $S_{\text{tot}}$ , indicating that sufficient sulfate is present. Critically, the presence of potential sulfate-reducing bacteria was also confirmed by METAGENassist. However, peat itself, which was used as filling material in the PRB, is likely not a good substrate for this purpose, as other organic materials, such as compost, saw dust, or manure, are more efficiently degraded through microbial respiration (Eger, 1994; Powell et al., 1998). During PRB construction, those materials were not easily accessible at the treatment site due to the remoteness of the location. Nevertheless, metal concentrations found in groundwater generally showed a strong decrease after passing through the PRBs. While the observed removal efficiencies are still relatively high for PRBs as compared to other case studies (Powell et al., 1998), we still found soil Ni concentrations higher than the recommended level (89 ppm, industrial soil quality guideline; Canadian Council of Ministers of the Environment (CCME), 2014), leaving Ni as a potential residual concern at this site.

The design and installation of PRBs, especially in remote locations with poor accessibility, appears to be an attractive, cost-effective, passive technology (Powell et al., 1998; Thiruvengkatachari et al., 2008). Future PRB applications in similar environments and for similar scenarios should consider the modest tendency of Ni and Co to sorb to solids or precipitate as a part of secondary mineral phases. Stronger microbial activity might be induced by the use of more degradable organic matter in the construction of the PRB, for example, compost or sawdust provided by logging operations. The thickness of the PRB should be properly assessed to make sure that under the dominant groundwater flow conditions, the contaminated stream has sufficient time to react with the PRB medium. More importantly, in the case of an alkaline PRB, the amount of base-generating material (e.g., limestone) should be properly adjusted to the long-term acid generation potential of the waste stream. At the same time, the pH change should not induce detrimental changes in the surface environment, such as potential Fe or P limitation in plants (Wilkinson, 2000). Water isotope investigations suggest that precipitation at the site rapidly percolates through the waste rock pile and reaches the wetland without evaporation. Upgradient modifications, for example, the establishment of a dense vegetation cover, could help to slow down water infiltration and help to retain contaminated groundwater in the source area. At Cluff Lake, the waste rock pile is being revegetated (AREVA, 2013), and future observations might reflect the success of this measure. Measurements of conductivity and metal concentrations further suggest that the waste stream may be partially passing the PRBs and the creek leading to a metal signature at isolated locations (e.g., station 24). Deeper placement of the PRBs or the use of an underground funneling installation to guide the groundwater flow through the reactive medium would likely have enhanced the PRB performance.

## 5. Conclusions

Biogeochemical investigations of two alkaline PRBs indicated that at the time of investigation they were both efficiently removing U and Cu from groundwater. The pH and redox conditions were key drivers in promoting the binding of these elements to the solid phase (colloidal and bulk) and, in the case of U, would

allow for immobilization by (bio)reduction. While the PRBs are documented to have performed well in removing mobile metals such as Mn, Fe, Co, and Ni (AREVA, 2013) in the years after installation, a reduced removal efficiency was observed for these metals at the time of our investigation. Presently, the groundwater quality guidelines/objectives are not being achieved for Mn, Fe, Ni, Co, and Zn, being 50, 300, 200, 50, and 30  $\mu\text{g/L}$ , respectively (CCME, 2014; Water Security Agency, 2015). Given the remoteness of the location, the risk of human exposure to this groundwater in form of agricultural or drinking water is rather low. However, exposure of the wetland to contaminants has resulted in Ni top soil concentrations above Canadian soil guidelines (CCME, 2014). This contamination can be transferred to macroflora and wildlife, potentially ending up in human receptors through fishing and hunting. Based on the historical development of contaminant concentrations (AREVA, 2013) and the current state of the PRBs, a lifetime of 5–10 years for this kind of system could be estimated, suggesting that after this time, no significant improvement in contaminant removal is achievable. However, such an estimate needs to be considered with caution given that the upgradient contaminant source is still active. Continuous long-term monitoring of this system, as well as the surrounding environments, is necessary to investigate the future development and potential contaminant remobilization at PRB sites.

### Acknowledgments

The authors acknowledge the support provided by Orano and CanNorth in terms of site access, sample collection, and borrowed equipment. Financial support was provided by the Natural Sciences and Engineering Research Council (Engage grant EGP 511159-17 to K. O. K.; Discovery grant RGPIN-04134 to D. S. A.) and by UAlberta North (University of Alberta Northern Research Award to K. v. G.). The authors also appreciate the assistance with the stable isotopes of water provided by Casey Buchanan and Duane Froese and the technical support by Katie Nichols. Raw 16S rRNA sequence reads can be accessed through to the NCBI database with the accession number PRJNA513194. Additional tables and figures can be found in the supporting information. We thank the two anonymous reviewers, whose comments helped to improve this work.

### References

- Adams, J. A., Osmond, J. K., & Rogers, J. J. (1959). The geochemistry of thorium and uranium. *Physics and Chemistry of the Earth*, 3, 298–348. [https://doi.org/10.1016/0079-1946\(59\)90008-4](https://doi.org/10.1016/0079-1946(59)90008-4)
- Alessi, D. S., Lezama-Pacheco, J. S., Janot, N., Suvorova, E. I., Cerrato, J. M., Giammar, D. E., et al. (2014). Speciation and reactivity of uranium products formed during in situ bioremediation in a shallow alluvial aquifer. *Environmental Science & Technology*, 48(21), 12842–12850. <https://doi.org/10.1021/es502701u>
- Altschul, S. F., Gish, W., Miller, W., Myers, E. W., & Lipman, D. J. (1990). Basic local alignment search tool. *Journal of Molecular Biology*, 215(3), 403–410. [https://doi.org/10.1016/S0022-2836\(05\)80360-2](https://doi.org/10.1016/S0022-2836(05)80360-2)
- AREVA (2013). Cluff Lake project: 2012 annual report. Technical report. AREVA Resources Canada Inc.
- Arndt, D., Xia, J., Liu, Y., Zhou, Y., Guo, A. C., Cruz, J. A., et al. (2012). METAGENassist: A comprehensive web server for comparative metagenomics. *Nucleic Acids Research*, 40(Web Server issue), W88–W95. <https://doi.org/10.1093/nar/gks497>
- Balk, M., Altunbaş, M., Rijpstra, W. I. C., Damste, J. S. S., & Stams, A. J. (2008). *Desulfatirhabdium butyratorvorans* gen. nov., sp. nov., a butyrate-oxidizing, sulfate-reducing bacterium isolated from an anaerobic bioreactor. *International Journal of Systematic and Evolutionary Microbiology*, 58(1), 110–115. <https://doi.org/10.1099/ijs.0.65396-0>
- Basiliko, N., & Yavitt, J. B. (2001). Influence of Ni, Co, Fe, and Na additions on methane production in *Sphagnum*-dominated Northern American peatlands. *Biogeochemistry*, 52(2), 133–153. <https://doi.org/10.1023/A:1006461803585>
- Benner, S. G., Blowes, D. W., Gould, W. D., Herbert, R. B., & Ptacek, C. J. (1999). Geochemistry of a permeable reactive barrier for metals and acid mine drainage. *Environmental Science & Technology*, 33(16), 2793–2799. <https://doi.org/10.1021/es981040u>
- Blowes, D. W., Ptacek, C. J., Benner, S. G., McRae, C. W., Bennett, T. A., & Puls, R. W. (2000). Treatment of inorganic contaminants using permeable reactive barriers. *Journal of Contaminant Hydrology*, 45(1-2), 123–137. [https://doi.org/10.1016/S0169-7722\(00\)00122-4](https://doi.org/10.1016/S0169-7722(00)00122-4)
- Borch, T., Kretzschmar, R., Kappler, A., Cappellen, P. V., Ginder-Vogel, M., Voegelin, A., & Campbell, K. (2010). Biogeochemical redox processes and their impact on contaminant dynamics. *Environmental Science & Technology*, 44(1), 15–23. <https://doi.org/10.1021/es9026248>
- Bouanane-Darenfed, A., Fardeau, M. L., & Ollivier, B. (2014). The family Caldicoprobacteraceae. In E. Rosenberg, E. F. DeLong, S. Lory, E. Stackebrandt, & F. Thompson (Eds.), *The prokaryotes*, (pp. 13–17). Berlin, Heidelberg, Germany: Springer. [https://doi.org/10.1007/978-3-642-30120-9\\_395](https://doi.org/10.1007/978-3-642-30120-9_395)
- Canadian Council of Ministers of the Environment (2014). Canadian environmental quality guidelines. Online database. Retrieved July 2019. <http://st-ts.ccme.ca/en/index.html>
- Canadian Nuclear Safety Commission (2003). Comprehensive study report, Cluff Lake decommissioning project. Canadian Nuclear Safety Commission.
- Cuss, C. W., Grant-Weaver, I., & Shoty, W. (2017). AF4-ICPMS with the 300 Da membrane to resolve metal-bearing “colloids” < 1 kDa: Optimization, fractogram deconvolution, advanced quality control. *Analytical Chemistry*, 89(15), 8027–8035. <https://doi.org/10.1021/acs.analchem.7b01427>
- Dai, M., Martin, J. M., & Cauwet, G. (1995). The significant role of colloids in the transport and transformation of organic carbon and associated trace metals (Cd, Cu and Ni) in the Rhône delta (France). *Marine Chemistry*, 51(2), 159–175. [https://doi.org/10.1016/0304-4203\(95\)00051-R](https://doi.org/10.1016/0304-4203(95)00051-R)
- Dean, J. A. (1999). *Lange's handbook of chemistry*, (15th ed.). New York, NY, USA: McGraw-Hill, Inc.
- Dise, N. B., & Verry, E. S. (2001). Suppression of peatland methane emission by cumulative sulfate deposition in simulated acid rain. *Biogeochemistry*, 53(2), 143–160. <https://doi.org/10.1029/2007JG000501>
- Domenico, P. A., & Schwartz, F. W. (1990). *Physical and chemical hydrogeology*. New York, USA: John Wiley & Sons.
- Dong, X., Kleiner, M., Sharp, C. E., Thorson, E., Li, C., Liu, D., & Strous, M. (2017). Fast and simple analysis of MiSeq amplicon sequencing data with MetaAmp. *Frontiers in Microbiology*, 8, 1461. <https://doi.org/10.3389/fmicb.2017.01461>
- Drake, H. L., Horn, M. A., & Wüst, P. K. (2009). Intermediary ecosystem metabolism as a main driver of methanogenesis in acidic wetland soil. *Environmental Microbiology Reports*, 1(5), 307–318. <https://doi.org/10.1111/j.1758-2229.2009.00050.x>
- Edgar, R. C. (2018). Updating the 97% identity threshold for 16S ribosomal RNA OTUs. *Bioinformatics*, 34(14), 2371–2375. <https://doi.org/10.1093/bioinformatics/bty113>
- Eger, P. (1994). Wetland treatment for trace metal removal from mine drainage: The importance of aerobic and anaerobic processes. *Water Science and Technology*, 29(4), 249–256. <https://doi.org/10.2166/wst.1994.0203>

- Gao, W., & Francis, A. J. (2008). Reduction of uranium (VI) to uranium (IV) by Clostridia. *Applied and environmental microbiology*, 74(14), 4580–4584. <https://doi.org/10.1128/AEM.00239-08>
- Gibson, J. J., Birks, S. J., Yi, Y., Moncur, M. C., & McEachern, P. M. (2016). Stable isotope mass balance of fifty lakes in central Alberta: Assessing the role of water balance parameters in determining trophic status and lake level. *Journal of Hydrology: Regional Studies*, 6, 13–25. <https://doi.org/10.1016/j.ejrh.2016.01.034>
- Glass, J., & Orphan, V. J. (2012). Trace metal requirements for microbial enzymes involved in the production and consumption of methane and nitrous oxide. *Frontiers in Microbiology*, 3, 61. <https://dx.doi.org/10.3389/fmicb.2012.00061>
- Golab, A. N., Peterson, M. A., & Indraratna, B. (2006). Selection of potential reactive materials for a permeable reactive barrier for remediating acidic groundwater in acid sulphate soil terrains. *Quarterly Journal of Engineering Geology and Hydrogeology*, 39(2), 209–223. <https://doi.org/10.1144/1470-9236/05-037>
- Graham, M. C., Oliver, I. W., MacKenzie, A. B., Ellam, R. M., & Farmer, J. G. (2011). Mechanisms controlling lateral and vertical porewater migration of depleted uranium (DU) at two UK weapons testing sites. *Science of the Total Environment*, 409(10), 1854–1866. <https://doi.org/10.1016/j.scitotenv.2011.01.011>
- Gustafsson, C., & Gschwend, P. M. (1997). Aquatic colloids: Concepts, definitions, current challenges. *Limnology and Oceanography*, 42(3), 519–528. <https://doi.org/10.4319/lo.1997.42.3.0519>
- Herbert, R. B. Jr., Benner, S. G., & Blowes, D. W. (2000). Solid phase iron–sulfur geochemistry of a reactive barrier for treatment of mine drainage. *Applied Geochemistry*, 15(9), 1331–1343. [https://doi.org/10.1016/S0883-2927\(00\)00005-6](https://doi.org/10.1016/S0883-2927(00)00005-6)
- Ho, Y. S., Wase, D. J., & Forster, C. F. (1996). Kinetic studies of competitive heavy metal adsorption by sphagnum moss peat. *Environmental Technology*, 17(1), 71–77. <https://doi.org/10.1080/09593331708616362>
- Honeyman, B. D. (1991). Surface chemistry, colloids and trace-element scavenging. In D. C. Hurd, & D. W. Spencer (Eds.), *Marine particles: Analysis and characterization*, (pp. 437–451). Washington DC: American Geophysical Union. <https://doi.org/10.1029/GM063p0437>
- Honeyman, B. D., & Santschi, P. H. (1991). Coupling adsorption and particle aggregation: Laboratory studies of “colloidal pumping” using iron-59-labeled hematite. *Environmental Science & Technology*, 25(10), 1739–1747. <https://doi.org/10.1021/es00022a010>
- Hong, H., Kim, S. J., Min, U. G., Lee, Y. J., Kim, S. G., Jung, M. Y., et al. (2015). *Geosporobacter ferrireducens* sp. nov., an anaerobic iron-reducing bacterium isolated from an oil-contaminated site. *Antonie van Leeuwenhoek*, 107(4), 971–977. <https://doi.org/10.1007/s10482-015-0389-3>
- Iino, T., Mori, K., Uchino, Y., Nakagawa, T., Harayama, S., & Suzuki, K. I. (2010). *Ignavibacterium album* gen. nov., sp. nov., a moderately thermophilic anaerobic bacterium isolated from microbial mats at a terrestrial hot spring and proposal of *Ignavibacteria* classis nov., for a novel lineage at the periphery of green sulfur bacteria. *International Journal of Systematic and Evolutionary Microbiology*, 60(6), 1376–1382. <https://doi.org/10.1099/ijs.0.012484-0>
- Illumina (2016). 16S Metagenomic sequencing library preparation. Retrieved October 2016. URL <https://pdfs.semanticscholar.org/bcd6/dc1196f3f906498d58aa39868895b18fa51d.pdf>
- Interstate Technology and Regulatory Council (2011). Permeable reactive barrier: Technology update. PRB-5. Washington, DC, USA: Interstate Technology & Regulatory Council, PRB: Technology Update Team. Retrieved June 2019. <https://www.itrcweb.org/GuidanceDocuments/PRB-5-1.pdf>
- Irving, H. M. N. H., & Williams, R. (1953). 637. The stability of transition-metal complexes. *Journal of the Chemical Society*, 3192–3210. <https://doi.org/10.1039/JR9530003192>
- Juottonen, H., Eiler, A., Biasi, C., Tuittila, E. S., Yrjälä, K., & Fritze, H. (2017). Distinct anaerobic bacterial consumers of cellobiose-derived carbon in boreal fens with different CO<sub>2</sub>/CH<sub>4</sub> production ratios. *Applied and Environmental Microbiology*, 83(4), e02533-16. <https://doi.org/10.1128/AEM.02533-16>
- Kämpfer, P., Young, C. C., Arun, A. B., Shen, F. T., Jäckel, U., Rossello-Mora, R., et al. (2006). *Pseudolabrys taiwanensis* gen. nov., sp. nov., an alphaproteobacterium isolated from soil. *International Journal of Systematic and Evolutionary Microbiology*, 56(10), 2469–2472. <https://doi.org/10.1099/ijs.0.64124-0>
- Kulichevskaya, I. S., Suzina, N. E., Liesack, W., & Dedysh, S. N. (2010). *Bryobacter aggregatus* gen. nov., sp. nov., a peat-inhabiting, aerobic chemo-organotroph from subdivision 3 of the Acidobacteria. *International Journal of Systematic and Evolutionary Microbiology*, 60(2), 301–306. <https://doi.org/10.1099/ijs.0.013250-0>
- Langmuir, D., & Herman, J. S. (1980). The mobility of thorium in natural waters at low temperatures. *Geochimica et Cosmochimica Acta*, 44(11), 1753–1766. [https://doi.org/10.1016/0016-7037\(80\)90226-4](https://doi.org/10.1016/0016-7037(80)90226-4)
- Li, W. C., Victor, D. M., & Chakrabarti, C. L. (1980). Effect of pH and uranium concentration on interaction of uranium (VI) and uranium (IV) with organic ligands in aqueous solutions. *Analytical Chemistry*, 52(3), 520–523. <https://doi.org/10.1021/ac50053a033>
- Libes, S. (2013). *Introduction to marine biogeochemistry* (2nd Ed.). Burlington, MA, USA: Academic Press.
- Lovley, D. R., & Phillips, E. J. (1986). Organic matter mineralization with reduction of ferric iron in anaerobic sediments. *Applied Environmental Microbiology*, 51(4), 683–689. PMID: 16347032
- Lovley, D. R., Roden, E. E., Phillips, E. J. P., & Woodward, J. C. (1993). Enzymatic iron and uranium reduction by sulfate-reducing bacteria. *Marine Geology*, 113(1-2), 41–53. [https://doi.org/10.1016/0025-3227\(93\)90148-0](https://doi.org/10.1016/0025-3227(93)90148-0)
- McMurdie, P. J., & Holmes, S. (2013). phyloseq: An R package for reproducible interactive analysis and graphics of microbiome census data. *PloS one*, 8(4), e61217. <https://doi.org/10.1371/journal.pone.0061217>
- Miyazaki, M., Koide, O., Kobayashi, T., Mori, K., Shimamura, S., Nunoura, T., et al. (2012). *Geofilum rubicundum* gen. nov., sp. nov., isolated from deep seafloor sediment. *International Journal of Systematic and Evolutionary Microbiology*, 62(5), 1075–1080. <https://doi.org/10.1099/ijs.0.032326-0>
- Newsome, L., Morris, K., Trivedi, D., Atherton, N., & Lloyd, J. R. (2014). Microbial reduction of uranium (VI) in sediments of different lithologies collected from Sellafield. *Applied geochemistry*, 51, 55–64. <https://doi.org/10.1016/j.apgeochem.2014.09.008>
- Oude Elferink, S. J. W. H., Visser, A., Pol, H., Look, W., & Stams, A. J. (1994). Sulfate reduction in methanogenic bioreactors. *FEMS Microbiology Reviews*, 15(2-3), 119–136.
- Päivänen, J. (1973). *Hydraulic conductivity and water retention in peat soils*. Hämeenlinna, Finland: Suomen metsätieteellinen seura. Arvi A. Karisto Osakeyhtiön kirjapaino.
- Parkhurst, D. L., & Appelo, C. A. J. (2013). *Description of input and examples for PHREEQC version 3: A computer program for speciation, batch-reaction, one-dimensional transport, and inverse geochemical calculations (No. 6-A43)*. Denver, CO, USA: US Geological Survey. Retrieved March 2019. <https://pubs.usgs.gov/tm/06/a43/>
- Patel, G. B., & Sprott, G. D. (1990). *Methanosaeta concilii* gen. nov., sp. nov. (“*Methanothrix concilii*”) and *Methanosaeta thermoacetophila* nom. rev., comb. nov. *International Journal of Systematic and Evolutionary Microbiology*, 40(1), 79–82. <http://doi.org/10.1099/00207713-40-1-79>



- Pham, S. V., Leavitt, P. R., McGowan, S., Wissel, B., & Wassenaar, L. I. (2009). Spatial and temporal variability of prairie lake hydrology as revealed using stable isotopes of hydrogen and oxygen. *Limnology and Oceanography*, *54*(1), 101–118. <https://doi.org/10.4319/lo.2009.54.1.0101>
- Poulton, S. W., & Canfield, D. E. (2005). Development of a sequential extraction procedure for iron: Implications for iron partitioning in continentally derived particulates. *Chemical geology*, *214*(3–4), 209–221. <https://doi.org/10.1016/j.chemgeo.2004.09.003>
- Powell, R. M., Blowes, D. W., Gillham, R. W., Schultz, D., Sivavec, T., Puls, R. W., et al. (1998). *Permeable reactive barrier technologies for contaminant remediation*. EPA/600/R-98/125. Washington, DC, USA: United States Environmental Protection Agency.
- Quevauviller, P., Rauret, G., & Griepink, B. (1993). Single and sequential extraction in sediments and soils. *International Journal of Environmental Analytical Chemistry*, *51*(1–4), 231–235. <https://doi.org/10.1080/03067319308027629>
- R Core Team (2017). *R: A language and environment for statistical computing*. Vienna, Austria: R Foundation for Statistical Computing. Retrieved November 2017. <https://www.R-project.org/>
- Rashid, M. A. (1974). Absorption of metals on sedimentary and peat humic acids. *Chemical Geology*, *13*(2), 115–123. [https://doi.org/10.1016/0009-2541\(74\)90003-5](https://doi.org/10.1016/0009-2541(74)90003-5)
- Rayment, G. E., & Higginson, F. R. (1992). *Australian laboratory handbook of soil and water chemical methods*. Melbourne, Australia: Inkata Press Pty Ltd.
- Rozanova, E. P., Nazina, T. N., & Galushko, A. S. (1988). Isolation of a new genus of sulfate-reducing bacteria and description of a new species of this genus, *Desulfomicrobium apsheronum* gen. nov., sp. nov. *Microbiology (Mikrobiologiya)*, *57*(5), 514–520.
- Sakai, K. (2015). Routine soil analysis using an Agilent 8800 ICP-QQQ. Application note 5991-6409EN. Agilent Technologies. [WWW document] Retrieved February 2018. URL <https://www.agilent.com/en-us/library/applications>
- Saunders, J. A., Lee, M. K., Dhakal, P., Ghandehari, S. S., Wilson, T., Billor, M. Z., & Uddin, A. (2018). Bioremediation of arsenic-contaminated groundwater by sequestration of arsenic in biogenic pyrite. *Applied Geochemistry*, *96*, 233–243. <https://doi.org/10.1016/j.apgeochem.2018.07.007>
- Scheller, S., Goenrich, M., Boecher, R., Thauer, R. K., & Jaun, B. (2010). The key nickel enzyme of methanogenesis catalyses the anaerobic oxidation of methane. *Nature*, *465*(7298), 606–608. <https://doi.org/10.1038/nature09015>
- Sela-Adler, M., Ronen, Z., Herut, B., Antler, G., Vigderovich, H., Eckert, W., & Sivan, O. (2017). Co-existence of methanogenesis and sulfate reduction with common substrates in sulfate-rich estuarine sediments. *Frontiers in Microbiology*, *8*, 766. <https://doi.org/10.3389/fmicb.2017.00766>
- Sheoran, A. S., & Sheoran, V. (2006). Heavy metal removal mechanism of acid mine drainage in wetlands: A critical review. *Minerals Engineering*, *19*(2), 105–116. <https://doi.org/10.1016/j.mineng.2005.08.006>
- Snape, I., Morris, C. E., & Cole, C. M. (2001). The use of permeable reactive barriers to control contaminant dispersal during site remediation in Antarctica. *Cold Regions Science and Technology*, *32*(2–3), 157–174. [https://doi.org/10.1016/S0165-232X\(01\)00027-1](https://doi.org/10.1016/S0165-232X(01)00027-1)
- Sorokin, D. Y., Rakin, A. L., Gumerov, V. M., Beletsky, A. V., Sinninghe Damsté, J. S., Mardanov, A. V., & Ravin, N. V. (2016). Phenotypic and genomic properties of *Chitinispirillum alkaliphilum* gen. nov., sp. nov., a haloalkaliphilic anaerobic chitinolytic bacterium representing a novel class in the phylum *Fibrobacteres*. *Frontiers in Microbiology*, *7*, 407. <https://dx.doi.org/10.3389%2Ffmicb.2016.00407>
- Stanek, W. (1973). Comparisons of methods of pH determination for organic terrain surveys. *Canadian Journal of Soil Science*, *53*(2), 177–183. <https://doi.org/10.4141/cjss73-028>
- Suzuki, Y., Kelly, S. D., Kemner, K. M., & Banfield, J. F. (2004). Enzymatic U (VI) reduction by *Desulfosporosinus* species. *Radiochimica acta*, *92*(1), 11–16.
- Tessier, A., Campbell, P. G., & Bisson, M. (1979). Sequential extraction procedure for the speciation of particulate trace metals. *Analytical Chemistry*, *51*(7), 844–851. <https://doi.org/10.1021/ac50043a017>
- Thiruvengkatchari, R., Vigneswaran, S., & Naidu, R. (2008). Permeable reactive barrier for groundwater remediation. *Journal of Industrial and Engineering Chemistry*, *14*(2), 145–156. <https://doi.org/10.1016/j.jiec.2007.10.001>
- Tran, E. L., Teutsch, N., Klein-BenDavid, O., & Weisbrod, N. (2018). Uranium and cesium sorption to bentonite colloids under carbonate-rich environments: Implications for radionuclide transport. *Science of the Total Environment*, *643*, 260–269. <https://doi.org/10.1016/j.scitotenv.2018.06.162>
- U.S. Environmental Protection Agency (1983). *Methods for Chemical Analysis of Water and Wastes*. EPA/600/4-79/020. Washington, DC, USA: Office of Research and Development. Retrieved November 2018. [https://www.wbdg.org/FFC/EPA/EPACRIT/epa600\\_4\\_79\\_020.pdf](https://www.wbdg.org/FFC/EPA/EPACRIT/epa600_4_79_020.pdf)
- Vail, J. (2013). *Groundwater sampling. Operating procedure*. Athens, Georgia: U.S. Environmental Protection Agency Science and Ecosystem Support Division. Retrieved June 2017. [www.epa.gov/sites/production/files/2015-06/documents/Groundwater-Sampling.pdf](http://www.epa.gov/sites/production/files/2015-06/documents/Groundwater-Sampling.pdf)
- Violante, A., Cozzolino, V., Perelomov, L., Caporale, A. G., & Pigna, M. (2010). Mobility and bioavailability of heavy metals and metalloids in soil environments. *Journal of Soil Science and Plant Nutrition*, *10*(3), 268–292. <https://doi.org/10.4067/S0718-95162010000100005>
- von Gunten, K., Alam, M. S., Hubmann, M., Ok, Y. S., Konhauser, K. O., & Alessi, D. S. (2017). Modified sequential extraction for biochar and petroleum coke: Metal release potential and its environmental implications. *Bioresource Technology*, *236*, 106–110. <https://doi.org/10.1016/j.biortech.2017.03.162>
- von Gunten, K., Hamilton, S. M., Zhong, C., Nesbø, C., Li, J., Muehlenbachs, K., et al. (2018). Electron donor-driven bacterial and archaeal community patterns along forest ring edges in Ontario, Canada. *Environmental Microbiology Reports*, *10*(6), 663–672. <https://doi.org/10.1111/1758-2229.12678>
- von Gunten, K., Warchola, T., Donner, M. W., Cossio, M., Hao, W., Boothman, C., et al. (2018). Biogeochemistry of U, Ni, As in two meromictic pit lakes at the Cluff Lake uranium mine, northern Saskatchewan. *Canadian Journal of Earth Sciences*, *55*(5), 463–474. <https://doi.org/10.1139/cjes-2017-0149>
- Wang, Q., & Riley, T. V. (2015). Chapter 47—Erysipelothrix rhusiopathiae. In Y. Tang, M. Sussman, D. Liu, I. Poxton, & J. Schwartzman (Eds.), *Molecular Medical Microbiology*, (2nd ed. pp. 859–872). Boston, MA, USA: Academic Press. <https://doi.org/10.1016/B978-0-12-397169-2.00047-0>
- Wang, Y., Frutschi, M., Suvorova, E., Phrommavanh, V., Descostes, M., Osman, A. A., et al. (2013). Mobile uranium (IV)-bearing colloids in a mining-impacted wetland. *Nature Communications*, *4*. <https://doi.org/10.1038/ncomms3942>
- Water Security Agency (2015). *Surface water quality objectives*. EPB 356. Regina, SK, Canada: Water Security Agency. <http://www.sask20.ca/pdf/epb356.pdf>
- Wilkinson, R. E. (Ed) (2000). *Plant-environment interactions*, (Vol. 77). Griffin, GA, USA: CRC Press.
- Yang, B., Tong, X., Deng, Z., & Lv, X. (2016). The adsorption of Cu species onto pyrite surface and its effect on pyrite flotation. *Journal of Chemistry*. <https://doi.org/10.1155/2016/4627929>



- Yang, K., Miao, G., Wu, W., Lin, D., Pan, B., Wu, F., & Xing, B. (2015). Sorption of  $\text{Cu}^{2+}$  on humic acids sequentially extracted from a sediment. *Chemosphere*, *138*, 657–663. <https://doi.org/10.1016/j.chemosphere.2015.07.061>
- Yilmaz, P., Parfrey, L. W., Yarza, P., Gerken, J., Pruesse, E., Quast, C., et al. (2014). The SILVA and “All-species Living Tree Project (LTP)” taxonomic frameworks. *Nucleic Acid Research*, *42*, D643–D648. <https://dx.doi.org/10.1093%2Fnar%2Fgkt1209>
- Yuan, X., Huang, H., Zeng, G., Li, H., Wang, J., Zhou, C., et al. (2011). Total concentrations and chemical speciation of heavy metals in liquefaction residues of sewage sludge. *Bioresource Technology*, *102*(5), 4104–4110. <https://doi.org/10.1016/j.biortech.2010.12.055>
- Yumoto, I., Hirota, K., & Nakajima, K. (2014). The genus *Alkalibacterium*. In W. H. Holzapfel, & B. J. B. Wood (Eds.), *Lactic acid bacteria: Biodiversity and taxonomy*, (pp. 147–156). Oxford, UK: John Wiley & Sons. <https://doi.org/10.1002/9781118655252.ch13>
- Zandvoort, M. H., Van Hullebusch, E. D., Feroso, F. G., & Lens, P. N. L. (2006). Trace metals in anaerobic granular sludge reactors: Bioavailability and dosing strategies. *Engineering in Life Sciences*, *6*(3), 293–301. <https://doi.org/10.1002/elsc.200620129>
- Zhang, K., Song, L., & Dong, X. (2010). *Proteiniclasticum ruminis* gen. nov., sp. nov., a strictly anaerobic proteolytic bacterium isolated from yak rumen. *International Journal of Systematic and Evolutionary Microbiology*, *60*(9), 2221–2225. <https://doi.org/10.1099/ijs.0.011759-0>